2.4. Storm Surge

An evaluation of the Probable Maximum Storm Surge (PMSS) flood hazard at MPS was performed in a manner consistent with the HHA approach (NRC, 2011). The evaluation included detailed analyses of the Probable Maximum Hurricane (PMH), the resulting deterministic stillwater elevation (i.e., the water surface elevation in the absence of waves, wave set-up and river flood PMSS) and the probabilistically-derived 1E-6 Annual Exceedance Probability (AEP) stillwater elevation.

To support the deterministic PMSS analysis, parameters defining the PMH were developed through a review of National Weather Service (NWS) guidance and a Site and Region Specific Hurricane Climatology Study, which included an analysis of a large set of synthetic hurricane data. Hydrodynamic modeling was then used to simulate the parameterized PMH and identify the resulting PMSS elevation at MPS.

The Site and Region Specific Hurricane Climatology Study also supported the evaluation of the 1E-6 AEP stillwater elevation by providing probabilistic definitions of key hurricane parameters. These definitions were used as input to a method of recovering combined event probabilities to evaluate the relationship between maximum stillwater elevation and AEP at MPS.

The methodology and results associated with the storm surge analysis at Surry Power Station (SPS) in Surry, Virginia were the subjects of an independent review performed by Dr. Donald T. Resio, Professor of Ocean Engineering at the University of North Florida. As the methodology used at SPS aligns with the approach taken with respect to assessing storm surge effects at MPS, Dr. Resio's review (i.e., methodology only) has been extended to be applicable to the approach described in the following sections (refer to Appendix D for further details with respect to the specific elements of this assessment to which the extended review is applicable). The favorable findings of the SPS review act to support the methods used to assess the PMSS flooding hazard at MPS.

2.4.1 Methodology

The following sections summarize the methodology used to evaluate the PMH, the deterministic stillwater PMSS elevation (i.e., deterministic storm surge) and the probabilistically-derived 1E-6 AEP stillwater PMSS elevation (i.e., probabilistic storm surge) at MPS.

2.4.1.1 Probable Maximum Hurricane

A step-wise approach consistent with HHA methodology, as described by NUREG/CR-7046 (NRC, 2011), was used to deterministically evaluate the PMH at MPS. The evaluation included analyses of National Hurricane Center (NHC) historical, "Best-Track" hurricane data (i.e., HURDAT2) and, to supplement the limited historical data, synthetic hurricane data representative of a large set of synthetic tropical cyclone tracks. The synthetic data were developed for the MPS region by Dr. Kerry Emanuel of WindRiskTech, LLC (WRT) using coupled intensity and atmospheric models (WRT, 2013). Details of the development methodology, comparisons with historical hurricane data and the application of extant methods are described in two key peer reviewed references (Emanuel et al, 2004; Emanuel et al 2006).

The methodology used to develop the synthetic tropical cyclone tracks and storm parameters includes: 1) storm generation; 2) storm track generation; and 3) deterministic modeling of

hurricane intensity. Using this methodology, a large number (10,013) of synthetic storm tracks (i.e., WRT storm set) was generated and filtered within a radius of 200 kilometers (km) of Westhampton, New York to support the evaluation of the PMH at MPS. The WRT storm set was verified by evaluating the statistical consistency with the HURDAT2 data set and, where present, variance from the historical hurricane data was identified. Comparisons were performed for parameters reflecting storm intensity, direction, size and speed. Based on these comparisons, the WRT data set was ultimately validated as a conservative reflection of storm characteristics within the MPS vicinity. Following validation, the WRT storm set was spatially filtered to eliminate data not reflective of conditions within the potential storm surge production region (i.e., filtered to include only over-water points within the 200 km radius zone)

The following steps were used to evaluate the historical and synthetic data and characterize the PMH at MPS:

1. Identification of controlling event type: hurricanes and extra-tropical storms are of primary concern in Atlantic coastal areas located in the regional area of MPS. The first step is to confirm which type of storm event (i.e. hurricane or extra-tropical storm) controls the PMSS. This evaluation is performed by: 1) reviewing recorded water level data from the NOAA Co-operative (Co Op) Stations at the Newport, Rhode Island (Station 8452660, "Newport"), New London, Connecticut (Station 8461490, "New London"), Bridgeport, Connecticut (Station 8467150, "Bridgeport") and Montauk, New York (Station 8510560, "Montauk") stations to identify the events that resulted in historical extreme water levels (Figure 2.4-1); 2) examining the extreme water levels predicted for Category 1 through Category 4 Hurricanes storm surge elevations by NOAA using the Sea, Lakes, and Overland Surges from Hurricanes (SLOSH) software model and presented in the NOAA SLOSH Display Program at the four NOAA Co-Op stations located near MPS relative to recorded water level data (NOAA 2012a); and 3) reviewing the historical hurricanes in the vicinity of MPS using historical storm data from the years 1851-2010 (Blake et al 2011 and NOAA 2013a).

2. Determine NWS-23 PMH parameters: consistent with guidance presented in NUREG/CR-7046 (NRC, 2011), ranges of permissible PMH meteorological parameters are initially determined using NWS-23 (NOAA 1979). These parameters include the following: 1) peripheral pressure, 2) central pressure, 3) permissible range for radius of maximum winds, 4) permissible range of forward speeds, 5) permissible range of track direction, and 6) estimated maximum 10-meter, 10-minute over-water wind speed of the key PMH parameters.

3. Site and Region Specific Hurricane Climatology Study: the Site and Region Specific Hurricane Climatology Study included a statistical analysis of the HURDAT2 database and verification and statistical analysis of the synthetically-developed hurricane parameter data set. The analysis focused on data reflecting storm intensity, direction and physical dimensions in the region of MPS. Parameter selection was based on data availability within the HURDAT2 database and relevance with respect to comparison to parameter estimates derived from NWS-23. Probability Density Functions (PDFs) were constructed for these parameters from Probability Density Histograms (PDHs) using a non-parametric kernel method. To further refine the analysis of the low probability portion of the 1-min, 10-m average wind speed (mxw) distribution, Extreme Value Analysis (EVA) was used based on the Peak Over Threshold (POT) method and the

Generalized Pareto Distribution (GPD). A detailed statistical analysis of the filtered WRT storm data was then performed including a univariate storm parameter probability analysis, an analysis of storm parameter covariance, development of a large synthetic storm set extension (i.e., the 3,000,000 or 3M data set), and an evaluation of error, uncertainty, and conservatism. Based on this analysis, a dimensionless scaling function was developed to conservatively reflect the deterministic upper-limit of storm intensity (i.e., maximum wind speed) in the MPS vicinity in consideration of co-variability with storm direction (i.e., storm bearing). Additional relationships were also developed to characterize additional storm parameters (e.g., forward speed and radius of maximum winds) in consideration of parameter co-variability.

The above-described methodology provided input to the deterministic and probabilistic storm surge analyses described below.

2.4.1.2 Deterministic Storm Surge

A step-wise approach consistent with HHA methodology, as described by NUREG/CR-7046 (NRC, 2011), was used to deterministically evaluate the PMSS stillwater elevation at MPS. As discussed below, two different hydrodynamic models were applied in a phased approach.

A screening-level assessment was performed using the two-dimensional Sea, Lakes and Overland Surges from Hurricanes (SLOSH) computer model (NOAA 2012a and NOAA 2012b). SLOSH is computationally efficient, allowing many simulations to be performed over a relatively short period of time; however, the SLOSH model has limitations, including its relatively coarse, structured model grid and the inability to represent dynamic tides and external boundary fluxes (e.g., river flow). Therefore, in a second phase of modeling (i.e., refinement-level assessment), additional simulations were performed using the ADvanced CIRCulation (ADCIRC) model (USACE, 1994). While ADCIRC is not hindered by many of the limitations associated with SLOSH, the high-resolution, finite-element mesh and related high computational demand prevent broad applications (i.e., only a limited number of storm simulations is practicable in the context of a given analysis). Therefore, ADCIRC was applied in a targeted fashion (i.e., refinement-level assessment) to further evaluate the storms identified during the screening-level assessment as potentially causing large surges at MPS and develop the final PMSS stillwater elevations.

Inclusive of the phased modeling approach, the methodology included the following steps:

1. Generation of the Initial Storm Set: An Initial Storm Set was generated using the MPS PMH results as input. Hypothetical storm tracks were first created by combining 10 potential storm bearings (i.e., -60° to +30° in 10° intervals) with five potential landfall locations between NWS 23 Mile Posts 2550 and 2650 (NOAA 1979). The storm tracks were assigned maximum wind speeds based on the bearing-specific values identified in the MPS PMH. Each potential storm track was then expanded into a set of storms using the bearing-specific ranges of forward speed and radius of maximum wind. Each range was divided into finite units, and a unique hypothetical (i.e., synthetic) storm was created for each combination.

2. Calculation of the Antecedent Water Level: An Antecedent Water Level (AWL) was calculated using data obtained from the Newport, Rhode Island NOAA tidal gaging

station per applicable regulatory guidelines (NRC, 2011 and ANS, 1992). In accordance with these guidelines, observed monthly maximum tide data obtained over a continuous 21-year period (i.e., January 1, 1993 through December 31, 2013) were used to calculate the 10% exceedance high tide. A factor representing attenuation to the Watch Hill Point, Rhode Island subordinate station at the high tide condition was then applied, and cumulative Sea Level Rise (SLR) was then added to obtain the AWL.

3. Screening-Level Assessment (SLOSH): Screening-level storm surge simulations were performed using the SLOSH model, the Initial Storm Set and the AWL. These simulations were performed to identify: 1) the sensitivity of storm surge at MPS to different storm parameters (i.e., storm track, radius of maximum winds, etc.) as constrained by the PMH results; and 2) the specific combinations of storm parameters and storm tracks that result in the largest predicted storm surges at MPS, also constrained by the PMH results. The screening-level simulations performed using SLOSH assumed steady-state conditions (i.e., storm parameters were not varied from the initial specifications).

4. Selection of the Refinement Storm Set: A Refinement Storm Set was selected for ADCIRC simulations after processing the results of the screening-level assessment (i.e., SLOSH model predictions). Maximum simulated stillwater elevations were recovered from the model output at the MPS intake location. These simulated elevations were ranked and sorted, and storms within the Initial Storm Set resulting in SLOSH-simulated stillwater elevations exceeding an applied threshold of 20 feet relative to the North American Vertical Datum of 1988 or NAVD88 were identified and combined to form the Refinement Storm Set.

5. Refinement-Level Assessment (ADCIRC): Refined storm surge simulations were performed using ADCIRC and a representation of dynamic tidal fluctuations for storms indicated by the screening-level assessment (i.e., Step 2, above) to be representative of the PMH. A preliminary sensitivity analysis was performed to establish storm arrival timing such that maximum stillwater elevations were achieved at MPS within the model (i.e., storm surge combined with variations in tide). Simulations were performed assuming steady conditions similar to the screening-level assessment for the purpose of comparing ADCIRC to SLOSH.

The above-described methodology produced simulated stillwater elevations at a location within the ADCIRC model domain representative of the MPS intake location. Because dynamic tides were simulated based on astronomical/predicted tides (i.e., excluding meteorological effects and SLR), a final adjustment was made to linearly add the difference between the peak predicted tide and the calculated AWL. The results represent maximum predicted stillwater (i.e., without wind-wave action) PMSS elevations at MPS.

2.4.1.3 Probabilistic Storm Surge

A step-wise approach consistent with HHA methodology, as described by NUREG/CR-7046 (NRC, 2011), was used to probabilistically evaluate the PMSS stillwater storm surge elevations at MPS. Similar to the deterministic analysis described in the previous section, two different hydrodynamic models (i.e., SLOSH and ADCIRC) were used in a phased approach that

involved applications of the Joint Probability Method (JPM) and Joint Probability Methodology with Optimal Sampling (JPM-OS).

The JPM is a statistical method developed in the 1970s that is commonly used to probabilistically evaluate the coastal surge risk due to tropical cyclones (ESSA, 1970). The JPM utilizes a set of synthetic storms representing local climatology by combining individual storm meteorological parameters (e.g., intensity, bearing, forward speed, etc.), with each storm having a joint probability of occurrence calculated from the combined probability of each of the individual parameter probabilities. A frequency response relationship may then be derived from these parameter combinations and associated probabilities via a hydrodynamic model.

The most significant limitation associated with applying the JPM is the significant computational requirement; many simulations representing a large number of unique parameter combinations are required in order to characterize the JPM integral. This limitation is exacerbated when using more robust, higher-precision numerical hydrodynamic models that require more computational effort (i.e., longer simulation times). To address this limitation and facilitate the use of these more robust models, modified forms of the JPM that rely on characterizing storm parameter space with fewer simulations through Optimal Sampling (OS) techniques have been developed (FEMA, 2012).

The Joint Probability Method – Optimal Sampling, or JPM-OS, was developed to statistically characterize surge-frequency relationships in the same manner as the traditional JPM but using fewer storm surge simulations. By limiting the number of storm surge simulations required, a robust, computationally intensive storm surge model, such as ADCIRC, can be applied. The basic JPM OS concept is to: 1) define the complete surge-frequency curve using a computationally efficient surge model (i.e., the NOAA SLOSH model); 2) statistically represent the complete surge-frequency relationship using relatively few storms, based on the appropriate selection of storm parameters and an understanding of surge response to varying storm parameters; 3) perform storm surge simulations for the storm subset using a robust storm surge model (i.e., ADCIRC); and 4) extend the results of these simulations to define the surge-frequency relationship at MPS.

The JPM-OS Response Surface technique developed by the United States Army Corps of Engineers (USACE) and applied by the Federal Emergency Management Agency (FEMA) was used (FEMA, 2012). In this approach, parameter space is characterized primarily via interpolation and extrapolation based on a carefully-selected set of reference parameter combinations or synthetic storms, where parameter perturbations and sensitivity testing based on this reference set are used to evaluate response functions. In concept, the JPM-OS calculation involves two steps: 1) searching for a reference storm based on the proximity of the given subject storm parameter combination to reference storm parameters; and 2) applying best-estimated surge responses along the multi-dimensional space.

The steps used to evaluate response functions and apply the JPM and JPM-OS are described as follows:

1. Creation of the JPM Storm Set: Storm parameters, including storm bearing (i.e., translational direction, fdir), forward speed (fspd), radius of maximum winds (RMW) and maximum (i.e., 1-minute average at an altitude of 10 meters) wind speed (Vm) were combined to generate hypothetical storms. Each storm track (i.e., storm bearing and landfall location) was expanded into a set of storms by considering ranges of

forward speed, radius of maximum winds and maximum wind speed. Each range was discretized into units of 5 knots (kt), 5 nautical miles (nm) and 10 kt, respectively. This discretization process resulted in 8 potential values of forward speed ranging from 15 kt to 50 kt, 9 potential values of radius of maximum winds ranging from 15 nm to 55 nm, and 8 potential values of maximum wind speed ranging from 70 kt to 140 kt. A unique hypothetical storm was created for each combination of values, storm track direction and landfall location (i.e., 8 x 9 x 8 x 11 x 5 = 31,680 hypothetical storms). Joint probabilities based on simultaneous occurrences of the Fdir, Fspd, RMW and Vm parameters were calculated for each hypothetical storm by querying the 3M data set to recover parameter co-variability. Hypothetical storms with joint probabilities of zero (i.e., no events within the 3,000,000, or 3M, data set matching or exceeding the parameter combination; a joint probability of less than 3.33E-7 or less than 1 in 3,000,000) were eliminated; the remaining 13,485 parameter combinations represented the JPM Storm Set. This method of establishing limits on parameter combinations differs from use of the 3M data set in the evaluation of the PMH, where a dimensionless scaling relationship was derived to adjust the NWS 23 maximum wind speed in recognition of co-variability of intensity and storm bearing.

2. Addition of tidal condition: An initial condition (i.e., static starting water level) was required by SLOSH for each simulation in performing the JPM analysis. Mean High Water (MHW) and Mean Low Water (MLW) at the Newport, Rhode Island (RI) NOAA CO-OPS station attenuated to the Watch Hill Point, RI subordinate station were selected as being representative of high and low tide conditions at the site, respectively. Both conditions were conservatively represented as having equal occurrence probabilities of 0.5 (i.e., equal probabilities of a hypothetical storm occurring at conditions representative of high and low tides).

3. Calculation of Annual Exceedance Probabilities: Annual Exceedance Probability (AEP) values were calculated for each hypothetical storm based on the joint probabilities calculated during Step 2. To develop surge-frequency relationships reflecting annualized probabilities, two additional factors were considered. First, the joint probabilities were multiplied by a normalized (i.e., normalized per unit length of coastline within the study area) annual storm occurrence frequency (i.e., 0.20371 storms per year divided by 400 kilometers, or the diameter of the capture zone from the PMH evaluation). As a final adjustment, the annualized probabilities were multiplied by a factor of 0.5 to represent coincidence with a high or low tide condition. Thus, for each simulated JPM Storm Set event, the maximum stillwater surge event was assigned an AEP value representing the storm parameter combination, the annual storm frequency and the tidal condition.

4. Performance of SLOSH simulations: A total of 26,970 simulations (i.e., 13,485 JPM Storm Set events, each at a high and a low tide condition) were performed using the SLOSH model. These simulations were performed to: 1) develop a preliminary surge-frequency relationship at MPS based on potential hurricane parameter combinations constrained by the PMH results; and 2) identify the set of storms to be simulated with ADCIRC for the purpose of refining this surge-frequency relationship. Results of the SLOSH simulations were extracted in the form of maximum stillwater surge elevations at several SLOSH model cells including the cell representing MPS.

5. Generation of an initial stillwater surge-frequency relationship: As a first step in developing an initial stillwater surge-frequency relationship at MPS, histograms were created for the MPS location using maximum stillwater surge elevations and the associated AEP values produced during Step 7. Bin sizes were defined as increments (i.e., 0.5 feet [ft]) of stillwater surge elevation based on the results of a sensitivity analysis, and AEP values associated with the storms producing stillwater surge elevations falling into each bin were summed. The summed AEP values were then summed again from highest elevation bin to the lowest elevation bin to produce bin-specific cumulative AEP values. The stillwater surge elevations representing the center of each bin were then plotted versus their respective cumulative AEP values to generate an initial stillwater surge-frequency relationship at MPS.

6. Identification of the OS Storm Set: As previously noted, perhaps the most significant challenge associated with the JPM-OS (i.e., where OS refers to optimal sampling) technique used in this analysis is selecting the storm parameter combinations used to formulate the basis for evaluating surge response. To guide this selection process in the case of this analysis, experiments were performed using the initial surge-frequency relationship developed using SLOSH. The goal of the experiments was to identify the minimum number of storm parameter combinations required to reproduce (i.e., using JPM-OS) the surge-response relationship at MPS with reasonable accuracy. Ultimately, the experiments suggested that the very-low probability range of the surge-frequency relationship was accurately reproduced using 55 production runs spanning the -50° to +50° bearing range (i.e., the reference set) and 16 additional simulations to establish sensitivities to various parameter perturbations (i.e., the sensitivity set).

7. Performance of ADCIRC simulations: As a first step in refining the surge-frequency relationship at MPS, reference and sensitivity set parameter combinations identified during Step 9 were simulated using ADCIRC (i.e., a total of 71 simulations). Whereas initial conditions representative of high and low tide levels were specified as input to the SLOSH simulations, a mean tide initial condition was used for the ADCIRC simulations; coincidence between surge and fluctuating tides was addressed during final adjustments (i.e., refer to Step 9). Results of the ADCIRC simulations were extracted in the form of maximum stillwater surge elevations at a location within the ADCIRC mesh representative of the MPS intake.

8. Refinement of stillwater surge-frequency relationships: A refined stillwater surge-frequency relationship was developed for MPS based on the results of the ADCIRC simulations using the JPM-OS technique. Maximum stillwater elevations were estimated via JPM-OS for an expanded set of storms (i.e., including two additional potential forward speeds: 5 and 10 kt) to support assessment of aleatory variability in maximum wind speeds (i.e., Step 9). AEP values were adjusted to correct for the use of a single initial condition (i.e., mean tide) prior to histogram development.

9. Adjustments to the surge-frequency relationship to reflect uncertainty, error and sea level rise: Adjustments to account for uncertainty (i.e., epistemic uncertainty and aleatory variability), error and projected sea level rise (SLR) were required in order to probabilistically characterize storm surge at MPS. The uncertainty adjustments considered the following factors: variability in tide occurring coincident with maximum storm surge; model skill associated with ADCIRC and the applied wind/vortex

formulation; and aleatory variability and error associated with maximum wind speed specifications. A uniform adjustment for SLR was added linearly as a final step.

The above-described methodology produced an estimated stillwater surge-frequency relationship for MPS. The 1E-6 AEP stillwater elevation was then extracted from this relationship.

2.4.2 Results

2.4.2.1 Probable Maximum Hurricane

The following sections describe the results of the evaluation of the PMH at MPS.

2.4.2.1.1 Determination of the Controlling Storm Event

As Table 2.4-1 indicates, both extra-tropical storms and hurricanes have resulted in significant coastal storm surges at the four stations (i.e., Newport, New London, Bridgeport, and Montauk). The data indicate that three to four of the top five extreme water level events were caused by either a hurricane or tropical storm for the site vicinity. Figure 2.4-3 shows the historical storm tracks intersecting the area of interest, including those storms responsible for many of the recorded high water levels at the stations identified above.

Storm surge elevations predicted by NOAA (NOAA 2012a) using the SLOSH model for hurricanes ranging from Category 1 to Category 4 were compared to the historical water level data. The purpose of this comparison was to determine whether large hurricanes are expected to result in storm surges greater than those measured in the historical record resulting from extra-tropical storms. A comparison of the Maximum of MEOW (MOM, where MEOW represents Maximum Envelope Of Water) values presented in Table 2.4-2 to the recorded water levels in Table 2.4-1 indicates that historic extra tropical storms have caused storm surges similar to those predicted for simulated Category 1 or 2 hurricanes.

Table 2.4-2 also confirms that the recorded water levels resulting from historic hurricanes have caused storm surges similar to those predicted for simulated Category 2 and 3 hurricanes. By definition, the PMH is a "hypothetical steady state hurricane having a combination of values of meteorological parameters that will give the highest sustained wind speeds that can probably occur at a specified coastal location" (NOAA 1979). At higher hurricane category levels (i.e., Category 3 and above), the potential surge elevations predicted by NOAA significantly exceed historical water levels recorded at the CO-OPS stations.

Finally, the frequency of hurricane strikes on the U.S. East Coast was analyzed in the NWS NHC-6 using the data from 1851 to 2010. Of all hurricanes making landfall in the U.S., 0.7 percent struck New Jersey, 4.2 percent struck New York, 3.9 percent struck Connecticut and 3.2 percent struck Rhode Island. According to NHC-6, the coastline represented by these states was impacted by 6 major hurricanes (Category 3 or higher) between 1851 and 2010 (Blake et al 2011).

Some of these storms occurred prior to 1900, and as a result, many accounts do not include storm surge, tide values, central pressure, or other specific storm details. With respect to the storms that are well characterized by historical records, many weakened significantly or dramatically changed direction prior to reaching the MPS vicinity; therefore, only some of these

storms produced significant storm surges. For storms that did impact the subject area after 1900, available track information is shown in Figure 2.4-4.

Based on: 1) a review of historical extreme water level data from the NOAA CO-OPS stations; 2) an examination of the extreme water level events associated with predicted hurricane storm surge elevations produced by NOAA using the SLOSH model at the four NOAA CO-OPS stations located near MPS; and 3) a review of available historical storm information, it is concluded that a major hurricane (i.e., the PMH) will be the controlling storm resulting in the PMSS at MPS.

2.4.2.1.2 Determination of Hurricane Parameters from NWS-23

The location of MPS is shown in Figure 2.4-5 in relation to coastal distance intervals (i.e., mile posts) presented in NWS 23 (NOAA 1979). Storm surge at MPS is caused by surge generated within Long Island Sound and/or coastal storm surge developed to the east of Montauk. As indicated on Figure 2.4-5, MPS is located approximately between NWS 23 mile posts 2575 and 2650 (more specifically, mile post 2650 approximately represents the opening of Long Island Sound to the Atlantic Ocean), where coastal distance is measured in nautical miles from the Gulf of Mexico. Based on the location of MPS the following range of PMH parameters are as follows:

Parameter	Lower Limit	Upper Limit
Peripheral Pressure (millibar)	1020	1020
Central Pressure (millibar)	907.4	908.5
Radius of Max Winds (nautical miles)	13	32
Forward Speed (knots)	35	48
Track Direction (degrees)	80	190
1-min, 10-meter over water wind speed (miles per hour)	169.9	169.9

The methods of parameter development presented in NWS 23 are generally not consistent with the current state of knowledge for characterizing the PMH affecting the MPS vicinity. In specific reference to PMH intensity reflected by maximum wind speed, NWS 23 values are recognized as lacking a reflection of the relationship between storm direction and storm magnitude (i.e., co-variability). Thus, a detailed Site and Region Specific Hurricane Climatology study was performed to develop the hurricane meteorological parameters for analysis of flooding due to combined storm surge and wind-generated waves.

2.4.2.1.3 Site and Region Specific Hurricane Climatology Study

2.4.2.1.3.1 Statistical Analysis of Historical Data

Univariate Parameter Probability Analysis

Best track positions of tropical storms and hurricanes are maintained by the NHC in the annually-updated HURDAT2 database (NOAA 2013a). The official HURDAT2 database contains data representing cyclones occurring between 1851 and 2012. The analysis of the HURDAT2 database for the MPS study area used all applicable 1851-2012 storm data, including the 1979-2012 subset containing central pressure data.

As the focus is on land-falling storms in the vicinity of Southern Long Island (i.e., since these storms result in large storm surges at MPS), the HURDAT2 database was filtered to extract storm parameters associated with three zones of increasing spatial coverage, as shown in Figure 2.4-6, with the Inner Region (IR) representing storms occurring in the MPS site vicinity:

- The IR – 200 kilometer radius centered at Westhampton, New York;
- The Outer Region (OR) – 50° sector region extending 400 kilometers radially to the south-southeast of the IR center; and
- The Remote Region (RR) – 50° sector region extending 800 kilometers radially to the south-southeast of the IR center.

Probability Density Functions (i.e., PDFs) were developed for key hurricane parameters within the IR using a non-parametric kernel method. The resulting IR distributions were compared to similarly sized sample distributions developed by randomly drawing from the OR and RR. The difference between any IR sample distribution and the OR and RR distributions was evaluated to determine statistical consistency for the purpose of maximizing the sample population (i.e., determine if an expanded spatial filter could improve sample size without bias). The non-parametric estimate of the population PDF for maximum wind speed, mxw, for the IR is shown in Figure 2.4-7 as a line. The 90% confidence interval, indicated by gray shading, was estimated by randomly drawing sample sizes from the OR and RR equivalent to the IR population (i.e., N=25).

Comparisons between the IR PDFs and the corresponding OR and RR sample-based PDFs for the fdir, fspd, dmxw and cpd parameters are shown in Figure 2.4-8 through Figure 2.4-10. Much like the mxw comparison, substantial differences are evident between the IR PDF and the OR and RR populations.

With central pressures routinely recorded in the HURDAT2 database only after 1979, the sample sizes for analyzing central pressure and pressure tendencies are considerably reduced relative to the full dataset. For each mid-6-hour position in the three regions, the central pressure deficit, cpd, was conservatively calculated using a peripheral pressure of 1020 mb (30.12 in Hg). The resulting PDFs for the IR are compared to the OR and RR samples in Figure 2.4-10. Figure 2.4-11 presents the PDF and Probability Density Histogram (PDH) for maximum sustained winds inside the IR.

Because the HURDAT2 database contains tropical storm and hurricane data, all primary

distribution peaks correspond to cpd values of slightly greater than 20 mb (i.e., central pressure equal to 1000 mb). The PDF representing the distribution of cpd within the IR is bi-modal with a secondary peak at approximately 70 mb representing stronger storms. This separation in storm intensity probabilities within the IR represents an artifact of the limited sample size associated with this capture zone. In consideration of this result, the empirical distribution of the mxw parameter represents a preferable metric of storm intensity, as it has a much larger sample size.

In summary, these results suggest that the IR cannot be reliably expanded to increase the historical data sample size.

Hurricane Parameter Co-variability

The annual probabilities from the parameter-specific, univariate PDFs can be directly combined as a product to obtain joint probability estimates of various parameter combinations as long as the distributions can be demonstrated to be independent. If significant co-variability exists among the hurricane parameters, the probabilities of certain combinations may be different from the product of their independent probabilities.

A cross-correlation matrix of four hurricane parameters (mxw, fdir, fspd, dmxw) from data within the IR, OR and RR is shown in Figure 2.4-12. The statistical significance of each cross-correlation was determined in a manner similar to determining the significance of each parameter's distribution.

Although paired parameter correlations are quite low in general, many are statistically significant (i.e., highlighted in yellow). Scatter plots of the paired parameters in the off-diagonal elements of the cross-correlation matrix shown in Figure 2.4-12 are presented in Figure 2.4-13 through Figure 2.4-18 along with a least-squares estimate of each respective regression line. The figures are presented in order from least viable linear co-variability to most-viable co-variability, as assessed by visually inspecting the scatter of the parameter plotted on the ordinate axis along the range of the parameter plotted on the abscissa axis.

Figure 2.4-13 shows a complex co-variability of forward storm speed (fspd) and forward direction (fdir). The fastest moving storms are those moving toward the north and east (i.e., bearings between 0° and 90°); whereas, storms with strong eastward or westward motions typically move at slower speeds. This characteristic is consistent among the three sampled regions. Similarly, Figure 2.4-14 and Figure 2.4-15 indicate a strong non-linear relationship exists between the storm intensity, as measured by mxw, and forward storm direction (fdir) and forward speed (fspd), respectively. With the exception of one strong storm moving nearly due east, storms moving with strong eastward and westward motions are less intense compared to storms moving with northward or northeastward components, as indicated by Figure 2.4-14.

Figure 2.4-16, through Figure 2.4-18 show scatter plots of storm intensity change, as indicated by dmxw, versus forward direction (fdir), storm intensity (mxw) and forward speed (fspd), respectively. As indicated by Figure 2.4-16, the probability distributions of intensity changes are nonlinearly related to storm forward direction, at least in terms of the width of the distributions. Storms moving in north to northeastward directions exhibit broader intensity change distributions compared to the more westward and eastward moving storms. Within the IR, the

majority of storms are weakening when moving west of north.

Figure 2.4-17 indicates that distributions of intensity changes as functions of intensity bulge in width for moderately-strong storms and exhibit narrower spreads at lower and higher intensities. Figure 2.4-18 shows little variation in the breadth of the intensity change distribution with forward speed, and the small slope associated with the regression line suggests that this paired parameter set exhibits nearly independent co-variability.

The nonlinearity exhibited by the variation of the spread in one parameter in relation to the value of the second parameter is evident within all sampled regions. This finding argues against characterizing the co-variability by linear means. Also, in reference to Figure 2.4-13, which shows the relationship between fdir and fspd, treating these parameters as independent would produce artificially high probabilities that fast moving storms approach the IR with northeast or north-northeast bearings; a condition that is not consistent with the analysis of the HURDAT2 dataset.

In summary, the statistical analysis of historical data suggests that the IR cannot be reliably expanded to increase the historical data sample size. Furthermore, the data within the IR represent a small sample size for determining the joint probability of storm parameters, especially considering that many of the storms within the IR have made landfall south of the region and are passing inland prior to approaching the study area. Fortunately, validation and analysis of the synthetic WRT storm set, as presented below, indicates that parameter distributions are similar to those developed from historical data. Thus, the WRT storm set represents an acceptable basis for characterizing PMH parameters in the vicinity of MPS.

2.4.2.1.3.2 Statistical Analysis and Verification of Synthetic Hurricane Data

The synthetic storm set contains over 10,000 storms (i.e., tropical storms and hurricanes) characterized by various angles, translational speeds, intensities, and maximum wind radii. The storm parameters are available at 2-hr intervals and represent 10,013 storms pre-screened to impact the Long Island Sound area (i.e., the source of surge impacts to MPS). The pre-screening (i.e., limiting the synthetic storm set to storms with tracks that approach MPS within 200 km of Westhampton, New York) has an effect on the probability density distribution of some parameters; a fact that is considered in the validation of the data set.

Figure 2.4-19 through Figure 2.4-22 present the validation results for the hurricane parameters fdir, fspd, dmxw and mxw, respectively. Each figure contains three panels, showing distribution comparisons for the IR (top), OR (middle), and RR (lower) domains, respectively. The gray shaded region with the central gray line within each panel provides estimates of the WRT population distribution made from HURDAT2-sized sampling (i.e., sampling from the WRT storm set); whereas, the ten superimposed lines show PDFs calculated for the 10 HURDAT2 samples.

As noted through inspection of the figures referenced above, the results of the validation indicate that use of the WRT representation of the empirical storm data for estimating independent and joint variability of hurricane parameters will contain a conservative bias. While storm intensity is generally well-represented by the WRT data for major storms, the WRT's bias toward faster forward speeds and more westerly storms is expected, given the sensitivity to storm surge within the Long Island Sound vicinity, to conservatively predict more frequent and larger storm surges near MPS.

2.4.2.1.3.3 PMH Parameter Calculations

Following validation, the WRT storm set was used to statistically characterize storm parameters within the storm surge production region. The analysis was focused on data located primarily within the over-water area of the IR, referred to as the Offshore IR (OIR), as spatially filtering the data to include only over-water points will produce a conservative set of storm parameters to support storm surge modeling. Figure 2.4-23 shows the IR, the OIR and the reduced number of storms (i.e., 7,957) and 2-hr storm segments (i.e., 23,993) resulting from spatial filtering to the dimensions of the OIR versus the IR.

With a reduction in the number of storms relative to the IR, the annual frequency of storms within the OIR is also reduced, as are the numbers of hurricanes of various intensities.

Table 2.4-3 lists the numbers of storms and 2-hr storm segments for all storms and for the three major storm categories. Figure 2.4-24 shows the annual frequency of synthetic storms within the IR and OIR by year and as a 31-year average (i.e., the 1980 to 2010 period corresponding to the synthetic storm simulations).

Univariate PDFs of relevant hurricane parameters from the WRT storm set filtered to the storm surge production region are presented in Figure 2.4-25 through Figure 2.4-28. The vertical lines represent central points for each interval. The tabulated probability densities apply to all data values within the stated intervals centered on the central point values. The middle rows of the tabulated probabilities represent interval-integrated values, and the bottom rows of values represent the middle row values multiplied by the adjusted annual frequency of occurrence for the WRT storm set (i.e., 0.20371). This adjusted annual frequency of occurrence represents the average year-by-year frequency of occurrence of all synthetic storms (i.e., intersecting the OIR) during the period between 1980 and 2010 within the storm surge production region.

Using an extension of the WRT data set based on sampling from each univariate PDF developed for synthetic data within the OIR (i.e., the 3M data set), parameters and parameter ranges for the PMH at MPS were developed in recognition of parameter co-variability. PMH parameters were determined by identifying a dimensionless scaling function that recovered variability of the NWS 23 PMH maximum wind speed, as described below. While the process of identifying this scaling function involved probability calculations for parameter combinations (i.e., storm bearing and maximum wind speed), the resulting parameter combinations represent conservative deterministic PMH upper limits, as the NWS 23 PMH maximum wind speed is used as the basis of function development.

In developing the dimensionless scaling function, AEP values were first assigned to maximum intensities for 10° storm bearing increments spanning the potential PMSS-causing sector (i.e., 10° sectors centered at -60°, -50°, -40°,...+30°) by querying the 3M data set. Criteria based on upper and lower limits were assigned to reflect a considered bearing sector (e.g., greater than or equal to -25° and less than -15° for the 10° bearing sector centered at -20°). Then, the number of events within the 3M data set meeting these criteria (i.e., all parameters falling within the pre-defined bounds) was counted. Finally, the resulting count for each considered bearing sector was divided by the size of the data set (i.e., 3,000,000) to produce the joint probability associated with the parameter combination; the reciprocal of this probability multiplied by the OIR's annual storm frequency (i.e., 0.20371) was calculated to reflect the return period (i.e., reciprocal of the AEP) for each parameter combination.

For extracted values exceeding 96 kt, adjustments were performed to scale intensity results to account for error introduced by the kernel-based method of PDF generation. Scaling was performed by evaluating differences in intensity over the potential PMSS-causing sector (i.e., -60° to +30°) described by differences between the extreme value analyses of the WRT and 3M data. For a given data set rank, the intensity predicted by an extreme value analysis fit to the 3M data was increased to be consistent with the intensity predicted by the fit to the WRT data.

Finally, bearing-specific PMH intensities were calculated using the following steps:

1. Storm intensity variation with bearing was evaluated over the potential PMSS-causing sector (i.e., -60° to +30°) and the sector calculated from NWS 23 (i.e., -100° to 10°) by arbitrarily specifying data set ranks.

2. As indicated by Figure 2.4-29, the 10° bearing interval associated with the maximum intensity was identified as 10° (i.e., storms from the 3M data set with bearings greater than or equal to 5° and less than 15°).

3. Using the NWS 23 PMH maximum wind speed (i.e., 147.6 kt), the data set rank associated with the 3M data set intensity most closely matching this value for the 10° bearing interval was identified (i.e., the 19th highest intensity for this bearing sector, 148.4 kt). This rank recognizes NWS 23 as being a conservative representation of PMH intensity within the -60° to +30° bearing sector.

4. Using the PMH intensity and bearing rank, intensities were extracted from the 3M data set for the 10° bearing intervals spanning the potential PMSS-causing bearing sector (i.e. -60° to +30°).

A least-squares regression line (i.e., fifth-order polynomial anchored to 147.6 kt at the 10° bearing interval) was then applied, and bearing-specific PMH intensities (i.e., vm as a function of fdir) were extracted from the regression function (Figure 2.4-29). The considered bearing range includes storms with bearings between -60° and 30° to provide a bounding parameter set (i.e., relative to the anticipated PMH) inclusive of more intense, northerly-bound storms.

Ranges of the rmw and fspd parameters were developed on a bearing-specific basis using the 3M data set and the results of the intensity analysis presented above (Figure 2.4-30). In the case of rmw, upper and lower parameter bounds were assigned based on the relationship to intensity, which shows a trend toward smaller radius and tighter range as intensity increases. For fspd, upper and lower parameter bounds were assigned based on relationships to intensity and bearing, which indicate a general trend toward faster forward speed as bearing shifts from -60° to 30° and intensity increases.

Recommended PMH-level parameters and parameter ranges are presented in Table 2.4-4 over a range of bearings (+/- 5°, centered on 10° increments) to capture the storm that causes the PMSS on a bearing-specific basis. The parameter ranges for fspd and rmw reflect bounding conditions relative to the likely controlling (i.e., maximum surge-producing) event within each storm bearing range. The maximum wind speeds represent conservative PMH intensities in consideration of applicable uncertainty and error, as supported by the following:

- Conservative intensity bias of WRT storm set versus HURDAT2 data;

- Assessment of potential uncertainty associated with the WRT storm set; and
- Assessment of error introduced by non-parametric, kernel-based fit.

Thus, the revised parameters and parameter ranges presented represent a conservative assessment of the PMH and provide input to the deterministic PMSS evaluation at MPS. Similarly, the PDFs developed from the WRT data within the OIR represent conservative reflections of parameter occurrence likelihoods and provide input to the probabilistic storm surge evaluation at MPS.

2.4.2.2 Deterministic Storm Surge

The following sections describe the results of the deterministic evaluation of the PMSS at MPS.

2.4.2.2.1 Generation of the Initial Storm Set

Fifty storm tracks were created based on ten potential bearings and five potential landfall locations (Figure 2.4-31) to span the potential surge generation region in the MPS vicinity. Each track was then assigned a maximum intensity based on the bearing-specific maximum wind speed determined as part of the PMH analysis. Finally, the tracks were assigned to unique pairings of the remaining, discretized parameters (i.e., radius of maximum winds and forward speed) to create the Initial Storm Set of 1,395 hypothetical events, each with a unique storm identification (STORMID) number.

Whereas a single maximum wind speed was determined for each bearing, the radius of maximum winds and forward speed parameters were presented as ranges (i.e., with upper and lower bounds varying by bearing). Thus, in generating the Initial Storm Set, these ranges were finely discretized by multiples of 5 nm and 5 kt, respectively. The upper and lower bounds of the ranges determined as part of the PMH analysis do not necessarily correspond to multiples of 5 nm or 5 kt; therefore, in generating the Initial Storm Set, the ranges were rounded to the nearest multiple (i.e., to span each range)

2.4.2.2.2 Calculation of the Antecedent Water Level

In accordance with NUREG/CR-7046 (NRC, 2011), the PMSS is required to be evaluated coincidentally with an AWL equal to the ten percent exceedance high tide plus long term changes in sea level. The ten percent exceedance high tide is defined as the high tide level that is equaled or exceeded by ten percent of the maximum monthly tides over a continuous 21 year period. In accordance with ANSI/ANS-2.8-1992 (ANS, 1992), this tide can be determined from recorded tide data or from predicted astronomical tide tables.

The ten percent exceedance high tide was calculated using recorded monthly maximum tide elevations from the Newport station attenuated to the Watch Hill Point subordinate station. Using this approach, a value of 2.796 ft NAVD88 was obtained. In consideration of Sea Level Rise (SLR), which was projected over 50 years using the annual rate at the Newport, RI station, the AWL was determined to be 3.2 ft NAVD88.

2.4.2.2.3 Screening-Level Assessment (SLOSH)

As part of performing the screening-level assessment performed using the NOAA SLOSH model, results from the 1,395 simulations, in the form of simulated surge elevation time series for each simulation, were extracted at four locations within the pv2 basin, including the model

cell representing the MPS intake location (Figure 2.4-32 and Figure 2.4-33). The time series were reduced to peak surge elevations at these locations for each simulated storm. The storms responsible for the largest simulated surges at MPS were identified, as discussed in the following section.

Figure 2.4-34 and Figure 2.4-35 summarize the results at MPS in the form of three-dimensional surfaces depicting maximum stillwater elevations as functions of storm bearing and forward speed or radius of maximum winds, respectively. Figure 2.4-34 suggests limited sensitivity to forward speed with some notable response differences between northbound storms and storms bearing west-of-north; whereas, Figure 2.4-35 indicates significant sensitivity to the radius of maximum winds parameter but generally consistent behavior across the storm bearing range.

Based on these responses, storm surge at MPS appears to be maximized by large-radius, slow-moving, northbound storms capable of moving significant coastal surge into the eastern Long Island Sound region. Due to the location of the maximum winds within the idealized cyclones, simulated storm surge is also maximized by storms making landfall west of the Long Island Sound opening. These slow-moving storms are able to maintain momentum and route surge from the open ocean south and southeast of Long Island through the Long Island Sound opening and toward MPS.

2.4.2.2.4 Selection of the Refinement Storm Set

The results of the screening-level assessment were used to target specific storm parameter combinations resulting in the largest stillwater surge elevations at MPS for refinement using the ADCIRC model (i.e., refinement-level assessment, which was performed using the Refinement Storm Set). The parameter combinations associated with the Refinement Storm Set events are summarized in Table 2.4-5. As Table 2.4-5 table indicates, the 17 storms making up the Refinement Storm Set represent 6 different potential storm bearings, 1 potential landfall location, 5 potential forward speeds and 3 potential radii of maximum winds.

2.4.2.2.5 Refinement-Level Assessment (ADCIRC)

Prior to performing dedicated refinement simulations, a sensitivity analysis was performed to determine the appropriate storm arrival time relative to the tide phase at Newport and MPS that would produce the most conservative results (i.e., the highest stillwater elevations at MPS). Time of landfall was used as an indicator for storm arrival time in this analysis.

Five simulations were performed, each with a different time of landfall relative to high tide at New London and MPS. The results indicated that when a storm made landfall one hour later (02:00) than the time for peak tide at Newport (01:00), maximum water level was obtained at MPS. Therefore, the storm tide elevation was considered to be maximized when a storm made landfall one hour later than the peak tide at Newport.

Guided by the results of the tidal phasing sensitivity analysis, ADCIRC simulations were performed using input defining the 17 storms within the Refinement Storm Set. Based on these simulations, the following combination of storm parameters was identified as being responsible for the deterministic PMSS at MPS:

STORMID = 818

- Track Direction (Θ) = -30°;

- Landfall Mile Post = 2600 (Latitude 40.88°, Longitude -72.35°);
- Radius of Maximum Winds (Rmax) = 35 nm;
- Forward Speed (Vf) = 20 kt
- Maximum 1-min, 10-m Overwater Wind Speed (Vm) = 125.6 kt; and
- Central Pressure Deficit (CPD) = 107 mb.

The ADCIRC simulation representing this combination of parameters (i.e., STORMID 818) resulted in a maximum stillwater elevation of 23.3 ft MSL (i.e., reflecting linear adjustment to the AWL) at the MPS intake location. This deterministically-derived maximum stillwater elevation represents a conservative result in consideration of the following:

- Conservatisms associated with the deterministic PMH inputs, as previously discussed;
- Consideration of the sensitivity to tidal phasing and coincidence between peak simulated tide and maximum storm surge; and
- The conservative value of the AWL applied in this analysis.

2.4.2.3 Probabilistic Storm Surge

The following sections describe the results of the probabilistic evaluation of the PMSS at MPS.

2.4.2.3.1 Creation of the JPM Storm Set

As a first step in generating the JPM Storm Set, potential storm bearings were assessed to identify combinations likely to contribute to the low-probability range of the surge-frequency relationship at MPS. As low-probability surge responses (i.e., relatively high maximum stillwater surge elevations) were anticipated for storms with approximately northerly bearings based on storm surge sensitivities observed as part of the deterministic evaluation, the range of considered storm bearings was limited to -50° to +50°.

Storm bearings between -50° to +50° (i.e., in 10° intervals) were combined with landfall locations to create a set of 55 storm tracks (Figure 2.4-36). Each potential storm track was expanded into a set of storms by considering ranges of forward speed, radius of maximum winds and maximum wind speed. This discretization process resulted in 8 potential values of forward speed ranging from 15 kt to 50 kt, 9 potential values of radius of maximum winds ranging from 15 nm to 55 nm, and 8 potential values of maximum wind speed ranging from 70 kt to 140 kt. A unique synthetic storm, each identified with a unique STORMID number, was created for each combination of parameters including storm track direction and landfall location (i.e., 8 x 9 x 8 x 11 x 5 = 31,680 synthetic storms).

Joint probabilities were calculated for each synthetic storm in a manner that recovered parameter co-variability, as reflected within the 3M data set. Based on these calculations, 13,485 parameter combinations were identified as having non-zero joint probabilities (i.e., at

least one record within the 3M data set falling within the upper and lower parameter bounds on each parameter). These parameter combinations were isolated to create the JPM Storm Set.

2.4.2.3.2 Addition of Tidal Condition

Given the computational efficiency of the NOAA SLOSH model (i.e., as compared to the more robust but computationally cumbersome ADCIRC model), two bounding tidal conditions could be practically simulated. Mean High Water (MHW) and Mean Low Water (MLW) at the Newport, RI NOAA CO-OPS station attenuated to the Watch Hill Point, RI subordinate station were selected as being representative of bounding tidal conditions at MPS.

Each storm in the JPM Storm Set was split into two conditions: one version of the storm occurring coincidentally with the high tide (i.e., MHW) condition, and another version of the same storm occurring coincidentally with the low tide (i.e., MLW) condition. This process doubled the size of the JPM Storm Set (i.e., 13,485 to 26,970 unique parameter combinations).

2.4.2.3.3 Calculation of Annual Exceedance Probabilities

In order to convert joint probabilities to annual exceedance probabilities (AEPs), two additional factors were considered: the probability associated with the simulated tidal condition and the omni-directional annual storm occurrence rate. Each joint probability was first multiplied by 0.5 to represent the probability of occurrence for the associated simulation's tidal condition (i.e., high tide or low tide). Each modified value was then multiplied by an omni-directional annual storm occurrence rate, which considered annual storm frequency (i.e., determined from the analysis of the WRT storm set), the approximate length of evaluated coastline and storm track spacing.

2.4.2.3.4 SLOSH Simulations

A total of 26,970 SLOSH simulations were performed using input representing the reduced JPM Storm Set. In accordance with applicable guidance (e.g., NRC, 2013), storms were simulated as steady-state events (i.e., input parameters, including storm bearing, were not varied from the initial values prior to landfall). Time series extracted for each storm in the JPM Storm Set were reduced to peak simulated surge elevations at several locations within the pv2 basin, including the location representative of the MPS intake. These maximum simulated stillwater elevations were used to develop a preliminary stillwater surge-frequency relationship at MPS, as described below.

2.4.2.3.5 Generation of an Initial Stillwater Surge-Frequency Relationship

Using the SLOSH model results and the calculated AEP values, a preliminary stillwater surge frequency relationship was calculated for the MPS intake using the standard JPM (i.e., non-OS). The calculations included the following steps which align with FEMA methodology for surge frequency determination (FEMA, 2012). This step established the basis for reducing the JPM Storm Set to the OS Storm Set (i.e., required for implementation of JPM-OS with ADCIRC), as described below.

2.4.2.3.6 Identification of the OS Storm Set

As indicated by Figure 2.4-37, experiments performed using the SLOSH model suggested that the very-low probability ranges of the surge-frequency relationships were well-defined (i.e., lower than an AEP value of approximately 1E-6) by an OS Storm Set comprised of model-simulated surges produced by storms with bearings between -50° and +50°. Furthermore, the

experiments suggested that the stillwater surge-frequency relationship at MPS represented by the remaining parameter combinations could be accurately reproduced using 55 production runs spanning the -50° to +50° bearing range (i.e., the reference set) and 16 additional simulations to establish sensitivities (i.e., calculate derivative terms) to various parameter perturbations (i.e., the sensitivity set).

2.4.2.3.7 Performance of ADCIRC Simulations

Results of the ADCIRC simulations (i.e., OS Storm Set) were evaluated at several locations within the model mesh including the node representative of the MPS intake location. ADCIRC simulations were performed using a static initial condition (i.e., 0 ft NAVD88) approximately representative of a mean tide condition at MPS; whereas, SLOSH simulations for the entire JPM Storm Set were performed using two static initial conditions representative of high and low tide conditions. This difference was addressed during final adjustments to account for uncertainty. Simulated maximum stillwater elevations at the MPS intake location for the OS Storm Set – reference set are shown in Table 2.4-6; the corresponding OS Storm Set – sensitivity set results are shown in Table 2.4-7.

For the storms simulated using ADCIRC, the ADCIRC wind field profiles generally compared favorably to the SLOSH predictions. Where slight differences were evident (e.g., large distances from the storm centers), the comparisons indicated conservatism in the ADCIRC representation (i.e., ADCIRC is predicting higher wind speeds compared to SLOSH). These favorable comparisons support the utility of applying SLOSH as screening-level assessment tool.

2.4.2.3.8 Refinement of Stillwater Surge-Frequency Relationships

Based on the ADCIRC results described above, a refined stillwater surge-frequency relationship was developed for MPS. AEP values were revised to exclude the tidal adjustment factor (i.e., 0.5) in recognition of the representation of a mean tide condition versus high and low tide conditions. In addition to deriving the stillwater surge-frequency relationship from ADCIRC results as opposed to SLOSH results, two other methodological modifications were made at this stage:

1. Potential forward speeds of 5 and 10 kt were considered by extrapolating the fspd surge response at 15 kt. This was done to fully span the low range of the forward speed parameter given the relatively high independent probability of a slow-moving storm and the previously-identified inverse correlation between forward speed and peak surge for some storm bearings at MPS.

2. Stillwater surge elevations were estimated for every storm parameter combination without consideration of non-zero joint probability (i.e., expanded to include forward speeds of 5 and 10 kt). These elevation estimates were necessary in order to characterize aleatory variability, as discussed in the following section.

The surge-frequency relationship at MPS was finalized by assessing uncertainty and error and linearly adding projected SLR, as described in the following section

2.4.2.3.9 Adjustments to the Surge-Frequency Relationship to Reflect Uncertainty, Error and Sea Level Rise

Two forms of uncertainty were considered in this analysis: epistemic uncertainty and aleatory variability. The former form of uncertainty generally represents a "lack of understanding" of the

physics within the system (i.e., measurement uncertainty, model skill, etc.); whereas, the latter form of uncertainty is attributed to sample size limitations associated with empirical data and/or the existence of unresolved or unpredictable variations in system behavior (NRC, 2012). Error associated with characterizing maximum wind speeds was also considered by evaluating the difference between EVA fits to the WRT and 3M data sets (i.e., similar to the comparison made as part of the PMH evaluation).

The sources of significant uncertainty considered in this analysis included (note that the first two potential sources are examples of epistemic uncertainty, the third potential source is an example of aleatory variability and the final potential source an example of error):

1. uncertainty in representing tide occurring coincidentally with surge:

   The effect of this source of uncertainty was quantified based on datum analysis results at the Newport, RI NOAA CO-OPS station (NOAA, 2013b). This uncertainty accounts for tide variation from the simulated initial condition (i.e., 0 ft NAVD88). This difference was calculated as the attenuated difference between the Mean High Water (MHW) elevation and the simulated initial condition (i.e., NAVD88 datum).

2. bias or uncertainty in numerical surge and wind field models (i.e., ADCIRC):

   The effect of this source of uncertainty was quantified based on the results of ADCIRC verifications performed by GZA. To estimate the 95% confidence interval, the maximum absolute error calculated based on observed and simulated peak water levels was conservatively multiplied by a factor of 2.

3. uncertainty due to sampling (i.e., aleatory variability associated with maximum wind speed):

   This source of uncertainty is variable as a function of maximum wind speed. The effect was quantified based on random sampling (i.e., "bootstrapping") performed using maximum wind speed values from the 3M dataset.

4. error within the 3M data set (i.e., deviation from the WRT storm set) associated with maximum wind speeds above 96 kt:

   This source of error is also variable as a function of maximum wind speed. The effect was quantified based on a comparison of EVA fits to the 3M and WRT data sets.

Consistent with FEMA methodology (FEMA, 2012), this analysis considered only uncertainty which resulted in higher or more-probable surge results (i.e., added conservatism); therefore, all uncertainty terms were considered to be positive such that they increased calculated surge elevations

The final uncertainty-adjusted stillwater relationship at MPS is shown in Figure 2.4-38. In addition to the uncertainty adjustments described above, this relationship also reflects an

additional linear adjustment to account for the 50-year SLR projection at MPS. The same relationship, converted to the MSL vertical datum, is shown in Figure 2.4-39. Similar to the deterministic PMSS evaluation, the probabilistic storm surge results described above are conservative in consideration of the following:

- Conservatisms associated with the deterministic PMH inputs, as previously discussed;
- Conservatism added through SLOSH assessment to establish appropriate reference and sensitivity storm sets for use with JPM-OS; and
- Conservatism added through consideration of applicable uncertainty, error and SLR.

2.4.3 Conclusions

Deterministic Probable Maximum Storm Surge

The ADCIRC simulation representing this combination of parameters (i.e., STORMID 818) resulted in a maximum stillwater elevation of 23.3 ft MSL (i.e., reflecting linear adjustment to the AWL) at the MPS intake location. This elevation exceeds the existing design basis maximum stillwater PMSS elevations of 18.2 ft MSL for MPS2 and 19.7 ft MSL for MPS3; however, flood protection at MPS2 (i.e., via flood wall containment) extends to 22.0 ft MSL, and MPS3 is protected from storm surge by a site grade elevation of 24.0 ft MSL (Dominion 2014b and Dominion 2014a).

Probabilistic Storm Surge

At an AEP level of approximately 1E-6, the stillwater elevation at MPS is calculated to be 19.7 ft NAVD88. This elevation translates to 20.7 ft MSL. This elevation may be compared to the existing design basis stillwater elevations of 18.2 ft MSL for MPS2 and 19.7 ft MSL for MPS3; however, it is important to note that flood protection at MPS2 (i.e., via flood wall containment) extends to 22.0 ft MSL, and MPS3 is protected from storm surge by a site grade elevation of 24.0 ft MSL (Dominion 2014b and Dominion 2014a).

2.4.4 References

2.4.4-1 ANS 1992. "ANS/ANS-2.8-1992 – Determining Design Basis Flooding at Power Reactor Sites", American National Standards Institute/American Nuclear Society, 1992

2.4.4-2 Blake et al. 2011. "The Deadliest, Costliest, and Most Intense United States Tropical Cyclones from 1851 to 2010 (and Other Frequently Requested Hurricane Facts)", Blake, E.S., Landsea, C.W. and Gibney, E.J., National Hurricane Center, National Oceanic and Atmospheric Administration Technical Report NWS NHC-6, August 2011.

2.4.4-3 Dominion 2014a. Millstone Power Station Unit-3 Final Safety Analysis Report (MPS-3 FSAR), Revision 25.2.

2.4.4-4 Dominion 2014b. Millstone Power Station Unit-2 Final Safety Analysis Report (MPS-2 FSAR), Revision 30.2.

2.4.4-5 Emanuel et al. 2004. "Environmental Control of Tropical Cyclone Intensity", Emanuel, K., Des Autels, C., Holloway, C. and Korty, R., Journal of the Atmospheric Sciences, Vol. 61, 843-858, April 2004.

2.4.4-6 Emanuel et al. 2006. "A statistical-deterministic approach to hurricane risk assessment", Bull. Amer. Meteor. Soc., 19, 299-314, K. Emanuel, A., S. Ravela, E. Vivant, and C. Risi, 2006.

2.4.4-7 ESSA, 1970. "Joint probability of tide frequency analysis applied to Atlantic City and Long Beach Island, NJ", U.S.Department of Commerce, Environmental Science Service Administration, Weather Bureau, Myers, V.A., April 1970.

2.4.4-8 FEMA, 2012. "Operating Guidance No. 8-12, Joint Probability – Optimal Sampling Method for Tropical Storm Surge Frequency Analysis", U.S. Department of Homeland Security, Federal Emergency Management Agency, March, 2012.

2.4.4-9 NOAA 1979. "Meteorological Criteria for Standard Project Hurricane and Probable Maximum Hurricane Wind Fields, Gulf and East Coast of the United States", National Oceanic and Atmospheric Administration Technical Report NWS 23, September 1979.

2.4.4-10 NOAA 2012a. "SLOSH Display Program (1.65b)", National Oceanic and Atmospheric Administration, Evaluation Branch, Meteorological Development Lab, National Weather Service, January 2012.

2.4.4-11 NOAA 2012b. "SLOSH Model v3.97" National Oceanic and Atmospheric Administration, Evaluation Branch, Meteorological Development Lab, National Weather Service, January 2012.

2.4.4-12 NOAA 2013a. "Revised Atlantic Hurricane Database (HURDAT 2)", National Oceanic and Atmospheric Administration, National Hurricane Center, http://www.aoml.noaa.gov/hrd/hurdat/2011.html, Date accessed December and January, 2013, Date updated June 10, 2013.

2.4.4-13 NOAA 2013b. "Tides and Currents Datum Information: Newport, RI Station 8452660", http://tidesandcurrents.noaa.gov/datums.html?id=8452660, Date accessed September, 2014. Date updated October, 2013.

2.4.4-14 NRC 2011. "NUREG / CR–7046: Design Basis Flood Estimation for Site Characterization at Nuclear Power Plants", U.S. Nuclear Regulatory Commission, November 2011.

2.4.4-15 NRC 2012. "NUREG/CR-7134 - The Estimation of Very-Low Probability Hurricane Storm Surges for Design and Licensing of Nuclear Power Plants in Coastal Areas", U.S. Nuclear Regulatory Commission, October 2012.

2.4.4-16 NRC 2013. "JLD-ISG-2012-06: Guidance for Performing a Tsunami, Surge, or Seiche Hazard Assessment", U.S. Nuclear Regulatory Commission, Revision 0, January 2013.

2.4.4-17 USACE 1994. "ADCIRC: an advanced three-dimensional circulation model for shelves coasts and estuaries, report 2: user's manual for ADCIRC-2DDI", Westerink, J.J., C.A. Blain, R.A. Luettich, Jr. and N.W. Scheffner, 1994, Dredging Research Program Technical Report DRP-92-6, U.S. Army Engineers Waterways Experiment Station, Vicksburg, MS., 156p.

2.4.4-18 WRT 2013. Synthetic Hurricane Event Set, WindRiskTech, LLC, Chesapeake_ncep_renanalcal.csv, Chesapeake _ncep_reanalcal2.csv and Chesapeake _ncep_reanalcal_freq.csv, September, 2013.

Table 2.4-1: Top 10 Extreme Water Levels.

(a) Newport (Station 8452660)

Rank	Year	Date	Highest WL (feet, NAVD88)	Event Type	Event Name
1	1938	9/21/1938	11.27	H2	New England Hurricane of 1938
2	1954	8/31/1954	8.57	H2	Carol 1954
3	2012	10/29/2012	6.02	ET	Sandy 2012
4	1991	8/19/1991	5.79	H2	Bob 1991
5	1944	9/14/1944	5.77	H1	Not Named
6	1978	1/9/1978	5.41	N/A	N/A
7	1991	10/31/1991	5.07	TS	Not Named
8	1978	2/7/1978	5.06	N/A	N/A
9	1963	11/30/1963	5.06	N/A	N/A
10	1974	12/2/1974	5.05	N/A	N/A

(b) New London (Station 8461490)

Rank	Year	Date	Highest WL (feet, NAVD88)	Event Type	Event Name
1	1938	9/21/1938	8.74	H2	New England Hurricane of 1938
2	1954	8/31/1954	7.74	H2	Carol 1954
3	2012	10/30/2012	6.1	ET	Sandy 2012
4	1950	11/25/1950	5.74	N/A	Not Named
5	1944	9/14/1944	5.24	H1	Not Named 1944
6	1960	9/12/1960	5.04	H2	Donna 1960
7	1953	11/7/1953	4.94	N/A	Not Named
8	1991	10/31/1991	4.63	TS	Not Named 1991
9	2011	8/28/2011	4.6	TS	Irene 2011
10	1968	11/12/1968	4.54	N/A	Not Named

Table 2.4-1 continued:

(c) Bridgeport (Station 8467150)

Rank	Year	Date	Highest WL (feet, NAVD88)	Event Type	Event Name
1	2012	10/30/2012	9.2	ET	Sandy 2012
2	2011	8/28/2011	8.2	TS	Irene 2011
3	1992	12/11/1992	8.2	N/A	Nor'Easter 1992
4	1991	10/31/1991	7.54	TS	Not Named 1991
5	1980	10/25/1980	7.15	N/A	Not Named
6	1984	3/29/1984	6.77	N/A	Not Named
7	1985	9/27/1985	6.75	TS	Henri 1996
8	1996	10/19/1996	6.69	N/A	Not Named
9	1968	11/12/1968	6.68	N/A	Not Named
10	2007	4/16/2007	6.67	N/A	Nor'Easter 2007

(d) Montauk (Station 8510560)

Rank	Year	Date	Highest WL (feet, NAVD88)	Event Type	Event Name
1	1954	8/31/1954	6.87	ET	Carol 1954
2	2012	10/29/2012	5.49	TS	Sandy 2012
3	1978	2/6/1978	5.18	N/A	Blizzard of '78
4	1991	10/31/1991	4.76	TS	Not Named 1991
5	1950	11/25/1950	4.67	N/A	Great Appalachian Storm 1950
6	1953	11/7/1953	4.37	N/A	Not Named
7	1968	11/12/1968	4.27	TS	N/A
8	1972	2/19/1972	4.20	N/A	N/A
9	1992	12/11/1992	4.17	N/A	N/A
10	2010	12/27/2010	4.03	N/A	Not Named

Notes: 1. H1, H2 indicate Category 1 and Category 2 Hurricane, respectively.
2. TS indicates Tropical Storm; ET indicates Extra-tropical Storm.

Table 2.4-2: NOAA SLOSH MOM Water Levels at Selected Gage Locations.

NOAA CO-OP Station (No.)	SLOSH Grid Cell (pv2)	CAT 1	CAT 2	CAT 3	CAT 4
		(feet, NAVD88)			
Newport (8452660)	73 - 74	4.4	7.8	11.5	15.0
New London (8461490)	102 - 28	5.6	9.9	14.2	18.3
Bridgeport (8467150)	143 - 5	6.9	11.7	16.7	22.5
Montauk (8510560)	114 - 46	3.9	6.8	9.6	12.3

Note: 1. MOM elevations reflect a mean tide initial condition.

Table 2.4-3: Numbers of WRT storms and storm segments within the OIR, including classifications by Saffir-Simpson category.

OIR Region	storms	storm segments
All	7957	23993
>= Cat 3 (96)	106	164
>= Cat 4 (113)	11	16
>= Cat 5 (137)	1	1

Table 2.4-4: Recommended PMH-level parameters and parameter ranges

Storm Bearing	Maximum Wind Speed, vm	Forward Speed, fspd	Radius of Maximum Wind, rmw
-60°	107.1 kt	16.1 – 37.0 kt	10.6 – 37.7 nm
-50°	111.9 kt	17.4 – 40.4 kt	10.9 – 35.8 nm
-40°	118.3 kt	19.2 – 43.9 kt	11.2 – 33.3 nm
-30°	125.6 kt	21.2 – 44.2 kt	11.7 – 30.5 nm
-20°	133.2 kt	23.3 – 42.0 kt	12.1 – 27.5 nm
-10°	140.1 kt	25.3 – 40.0 kt	12.5 – 24.9 nm
0°	145.2 kt	26.7 – 38.4 kt	12.8 – 22.9 nm
10°	147.6 kt	27.3 – 37.7 kt	12.9 – 21.9 nm
20°	146.6 kt	27.1 – 38.0 kt	12.8 – 22.3 nm
30°	141.6 kt	25.7 – 39.5 kt	12.6 – 24.2 nm

Table 2.4-5: Refinement Storm Set parameters. Vm is maximum sustained wind speed; CPD is central pressure deficit; Rmax is radius of maximum wind.

STORM ID	Vm (kt)	CPD (mb)	Bearing (deg. from N)	Forward Speed (kts)	Rmax (kt)	Landfall Mile Post (via NWS 23)	Landfall Latitude (Dec. Degrees)	Landfall Longitude (Dec. Degrees)
818	125.6	107	-30	20	35	2600	40.88	-72.35
823	125.6	103	-30	25	35	2600	40.88	-72.35
828	125.6	99	-30	30	35	2600	40.88	-72.35
968	133.2	112	-20	20	30	2600	40.88	-72.35
973	133.2	108	-20	25	30	2600	40.88	-72.35
978	133.2	104	-20	30	30	2600	40.88	-72.35
983	133.2	99	-20	35	30	2600	40.88	-72.35
1058	140.1	112	-10	25	25	2600	40.88	-72.35
1063	140.1	107	-10	30	25	2600	40.88	-72.35
1138	145.2	120	0	25	25	2600	40.88	-72.35
1143	145.2	117	0	30	25	2600	40.88	-72.35
1148	145.2	112	0	35	25	2600	40.88	-72.35
1153	145.2	107	0	40	25	2600	40.88	-72.35
1218	147.6	125	10	25	25	2600	40.88	-72.35
1223	147.6	120	10	30	25	2600	40.88	-72.35
1228	147.6	116	10	35	25	2600	40.88	-72.35
1298	146.6	124	20	25	25	2600	40.88	-72.35

Table 2.4-6: Maximum simulated stillwater surge elevations associated with the OS Storm Set – reference set at the MPS intake location (SLOSH and ADCIRC results shown).

STORMID	SLOSH - MPS (ft NAVD88)	SLOSH - MPS (ft MSL)	ADCIRC - MPS (ft NAVD88)	ADCIRC - MPS (ft MSL)
1376	8.6	9.6	8.4	9.4
1377	10.6	11.6	10.3	11.3
1378	12.1	13.1	12.2	13.2
1379	9.7	10.7	8.9	9.9
1380	4.4	5.4	4.0	5.0
4256	7.9	8.9	7.5	8.5
4257	10.2	11.2	9.8	10.8
4258	12.2	13.2	12.3	13.3
4259	9.7	10.7	9.0	10.0
4260	4.8	5.8	3.7	4.7
7136	7.5	8.5	6.7	7.7
7137	10.0	11.0	9.5	10.5
7138	12.0	13.0	12.0	13.0
7139	9.7	10.7	8.7	9.7
7140	5.7	6.7	4.6	5.6
10016	7.3	8.3	6.2	7.2
10017	10.0	11.0	9.2	10.2
10018	11.6	12.6	11.4	12.3
10019	9.6	10.6	8.7	9.7
10020	6.4	7.4	5.4	6.4
12896	7.5	8.5	6.2	7.2
12897	10.0	11.0	8.9	9.9
12898	11.1	12.1	10.4	11.4
12899	9.5	10.5	8.4	9.3
12900	6.9	7.9	5.7	6.7
15776	7.8	8.8	6.3	7.3
15777	10.0	11.0	8.4	9.4
15778	10.6	11.6	9.3	10.3
15779	9.1	10.1	7.9	8.9
15780	7.4	8.4	6.0	7.0
18656	8.1	9.1	6.4	7.4
18657	9.9	10.9	7.9	8.9
18658	10.0	11.0	8.2	9.2
18659	8.9	9.9	7.3	8.3
18660	7.7	8.7	5.9	6.9
21536	8.4	9.4	6.4	7.4
21537	9.5	10.5	7.1	8.1
21538	9.6	10.6	7.3	8.3
21539	8.7	9.7	6.7	7.7
21540	8.0	9.0	5.9	6.8
24416	8.6	9.6	6.1	7.1
24417	9.0	10.0	6.0	7.0
24418	9.1	10.1	6.4	7.4
24419	8.5	9.5	5.9	6.9
24420	8.1	9.1	5.6	6.5
27296	8.3	9.3	5.1	6.1
27297	8.6	9.6	5.4	6.4
27298	8.6	9.6	5.7	6.7
27299	8.2	9.2	5.2	6.2
27300	8.1	9.1	5.1	6.1
30176	8.0	9.0	4.5	5.5
30177	8.2	9.2	4.8	5.8
30178	8.1	9.1	4.8	5.8
30179	7.8	8.8	4.6	5.6
30180	7.9	8.9	4.7	5.7

Table 2.4-7: Maximum simulated stillwater surge elevations associated with the OS Storm Set – sensitivity set at the MPS intake location (SLOSH and ADCIRC results shown). Note that STORMID = 12898 is used to evaluate parameter sensitivities (i.e., results associated with STORMID = 12898 are highlighted)

STORMID	SLOSH - MPS (ft NAVD88)	SLOSH – MPS (ft MSL)	ADCIRC - MPS (ft NAVD88)	ADCIRC - MPS (ft MSL)
12883	5.9	6.9	3.8	4.8
12888	7.3	8.3	5.6	6.6
12893	9.0	10.0	7.8	8.8
12903	13.5	14.5	13.1	14.1
12908	15.8	16.8	15.9	16.9
12818	10.8	11.8	10.9	11.9
12858	11.0	12.0	10.6	11.6
12898	11.1	12.1	10.4	11.4
12938	10.9	11.9	10.0	11.0
12978	10.9	11.9	9.6	10.6
13018	10.6	11.6	9.0	10.0
11618	6.8	7.8	6.2	7.2
11938	8.5	9.5	7.8	8.8
12258	9.4	10.4	8.9	9.9
12578	10.2	11.2	9.9	10.9
13218	11.7	12.7	10.7	11.7
13538	12.5	13.5	10.9	11.9

Figure 2.4-1: Site locus and NOAA tide gage locations.

Figure 2.4-2: Illustration of several key PMH parameters.

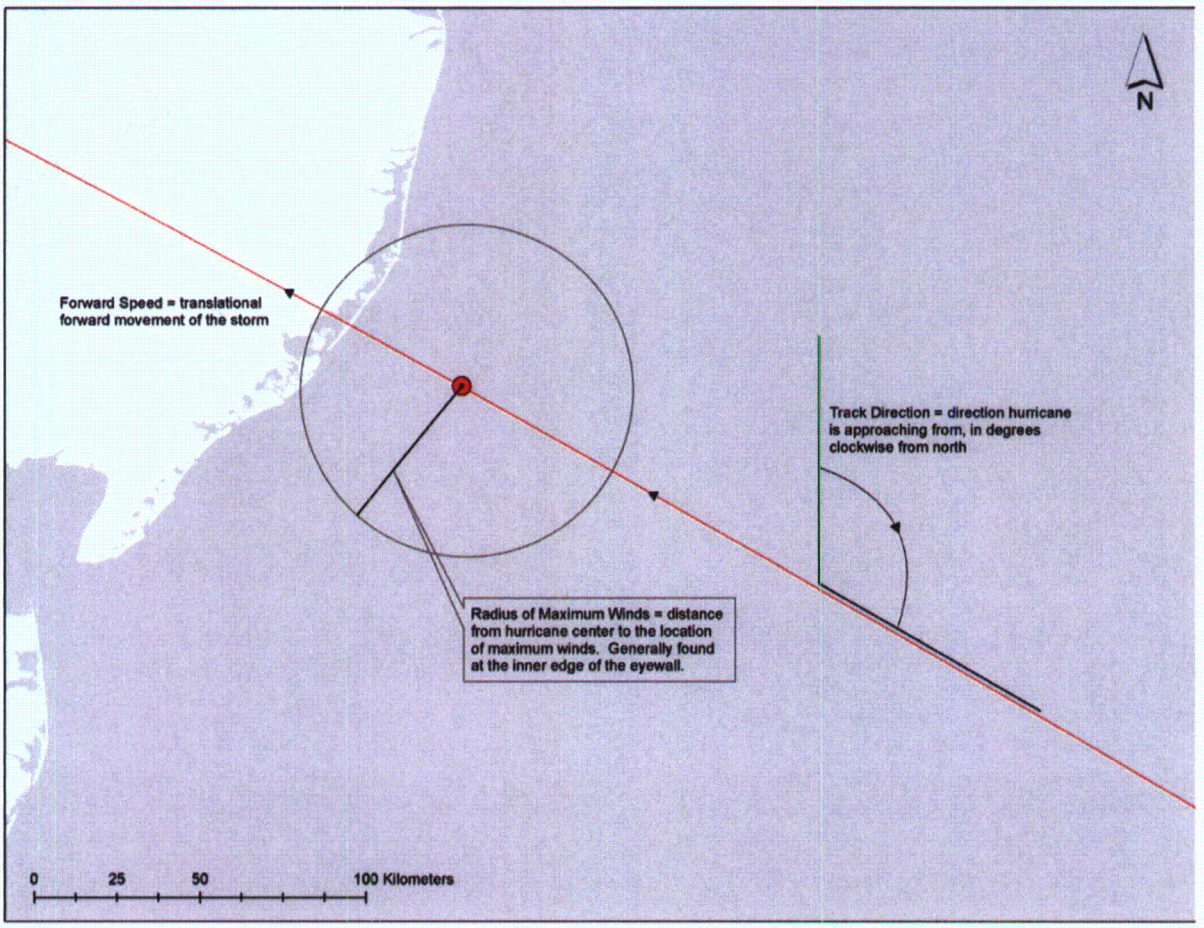

Figure 2.4-3: Historical hurricane tracks intersecting the study area (200 km radius from Westhampton, New York).

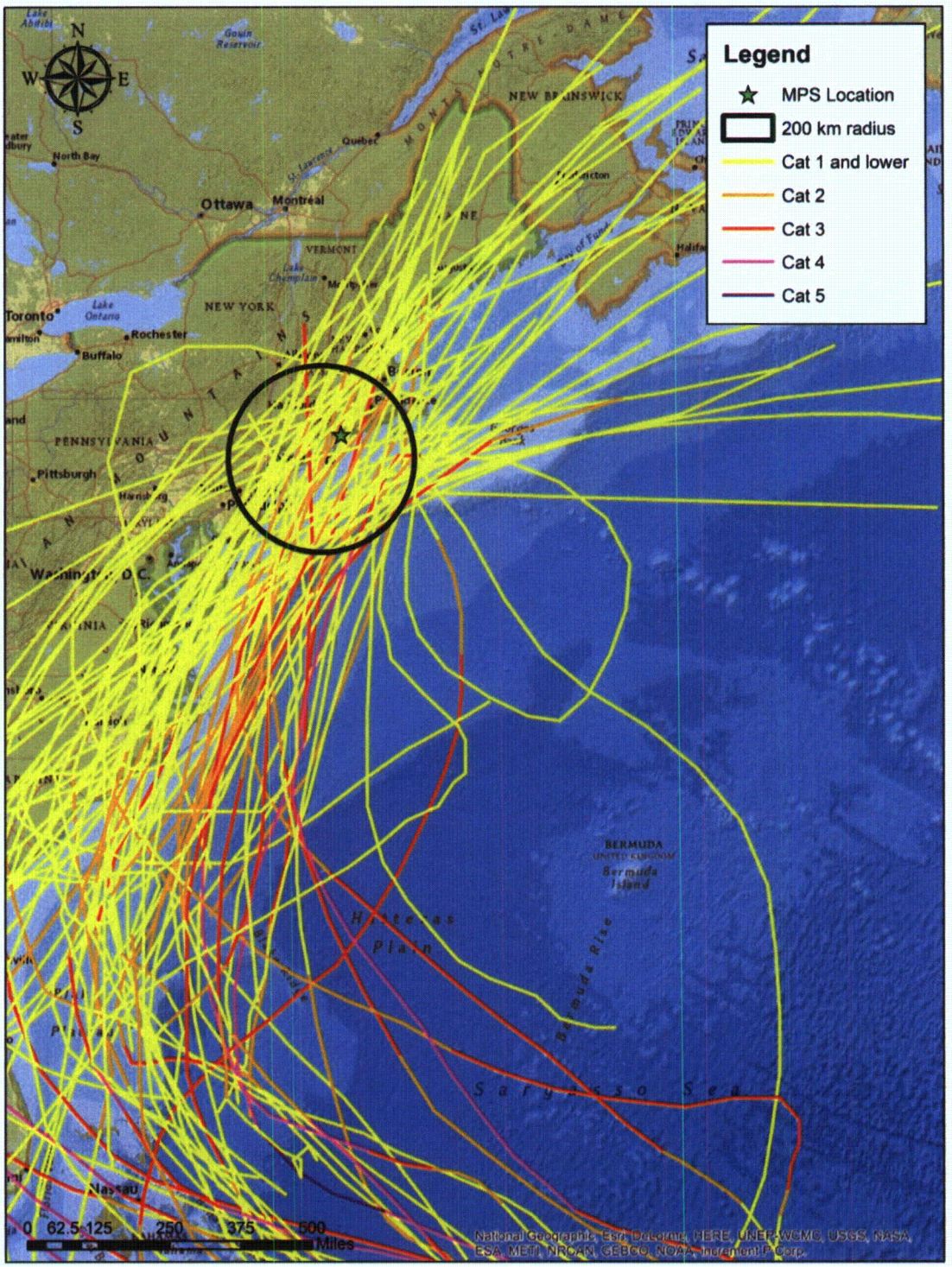

Figure 2.4-4: Selected historical hurricane tracks impacting the MPS vicinity.

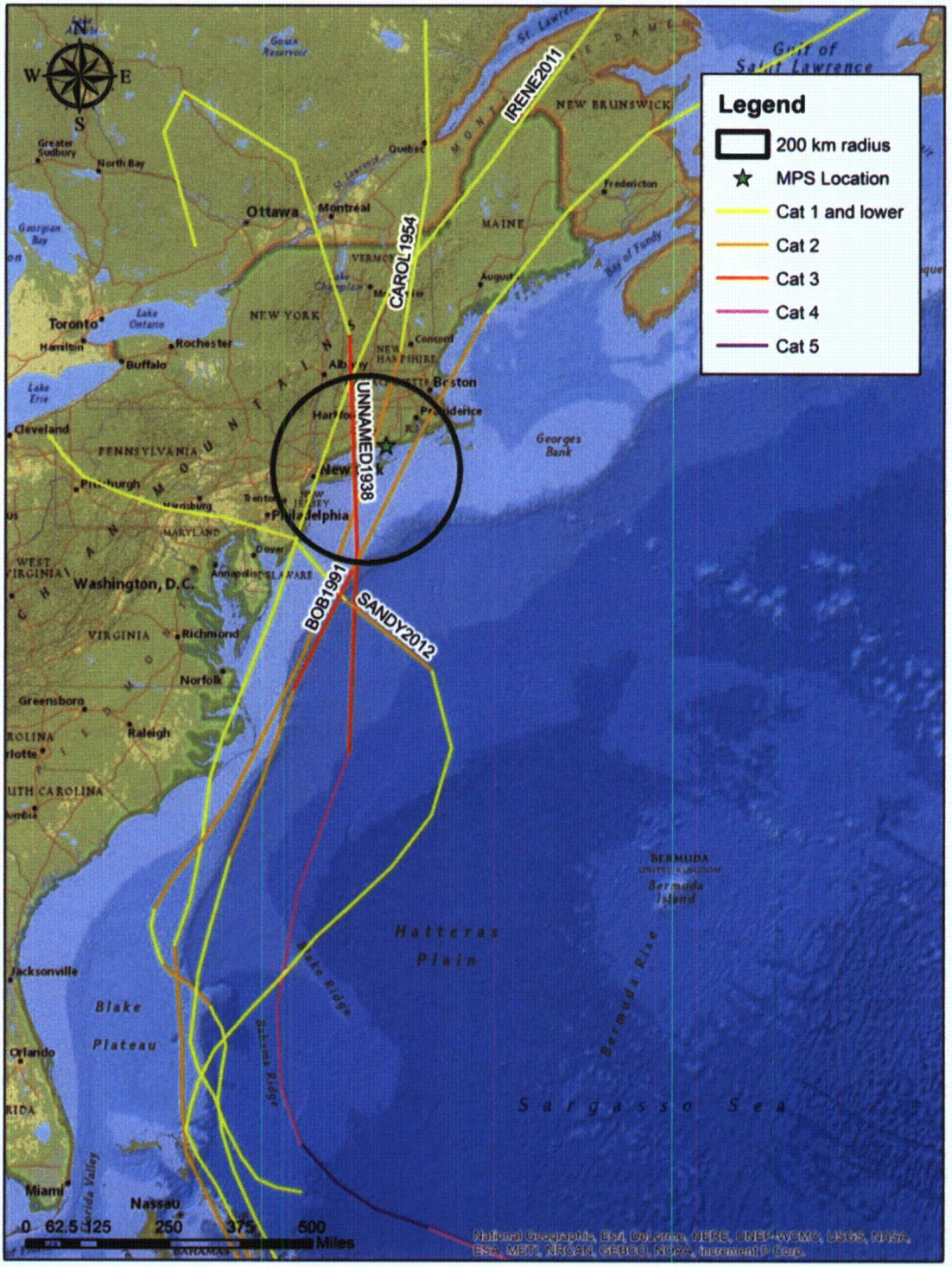

Figure 2.4-5: MPS mile post location (NWS 23, Figure 1.1). Adapted from NOAA 1979 (NOAA 1979).

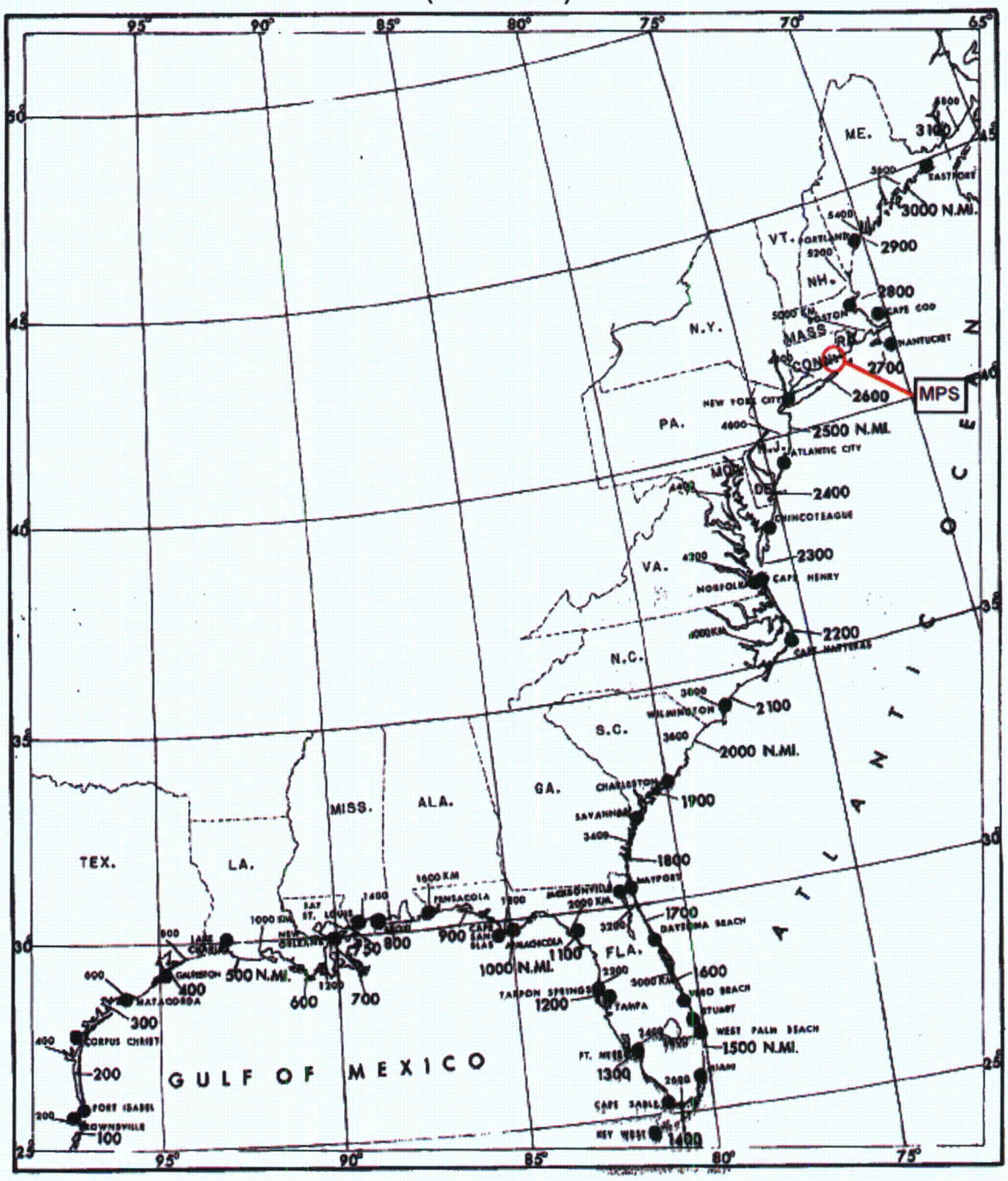

Figure 1.1.--Locator map with coastal distance intervals marked in nautical miles and kilometers.

Figure 2.4-6: Hurricane parameter sampling regions.

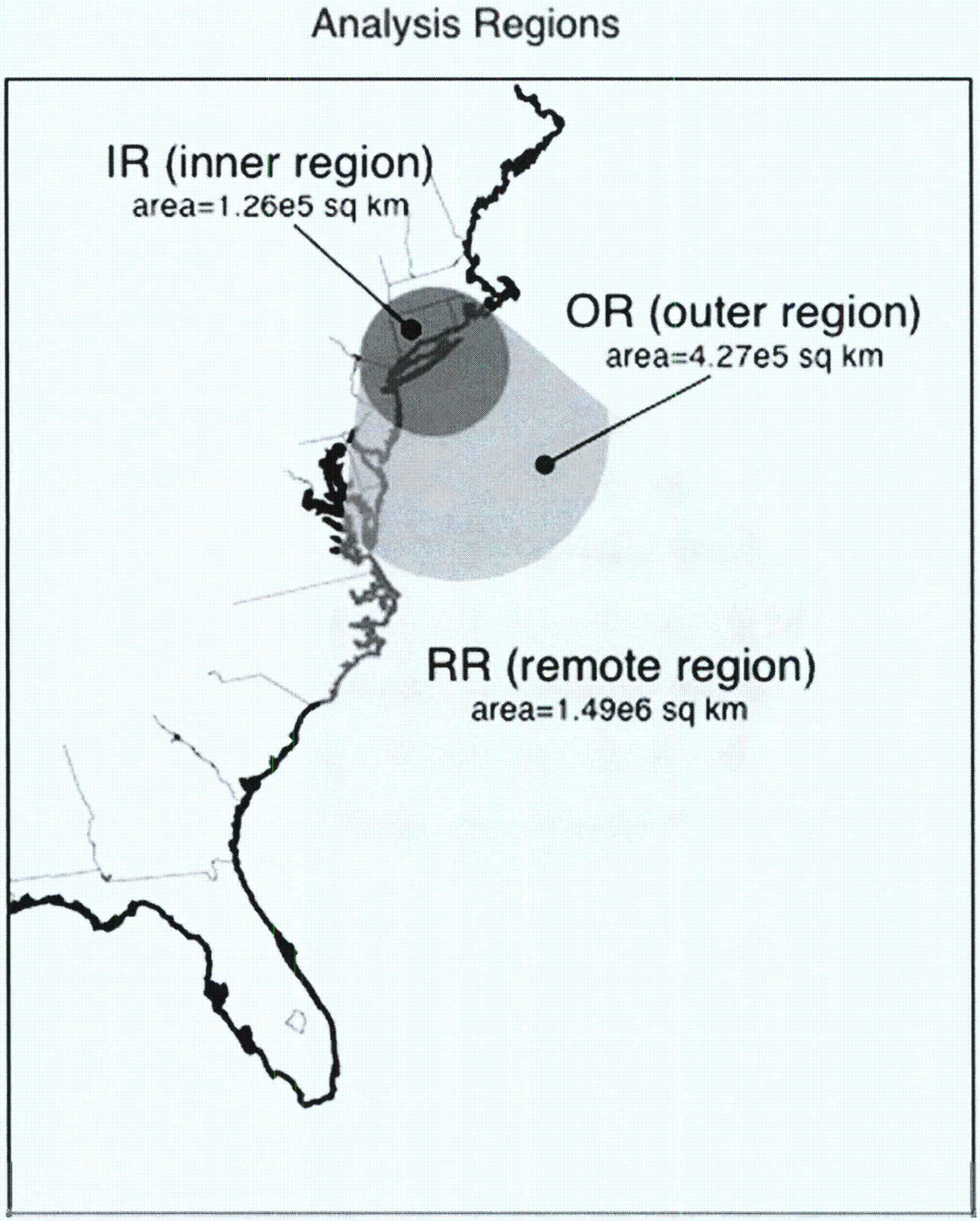

Figure 2.4-7: The PDF, CDF, tabulated probabilities and annual frequencies for the mxw parameter within the IR. The envelope PDFs pertain to the OR and RR.

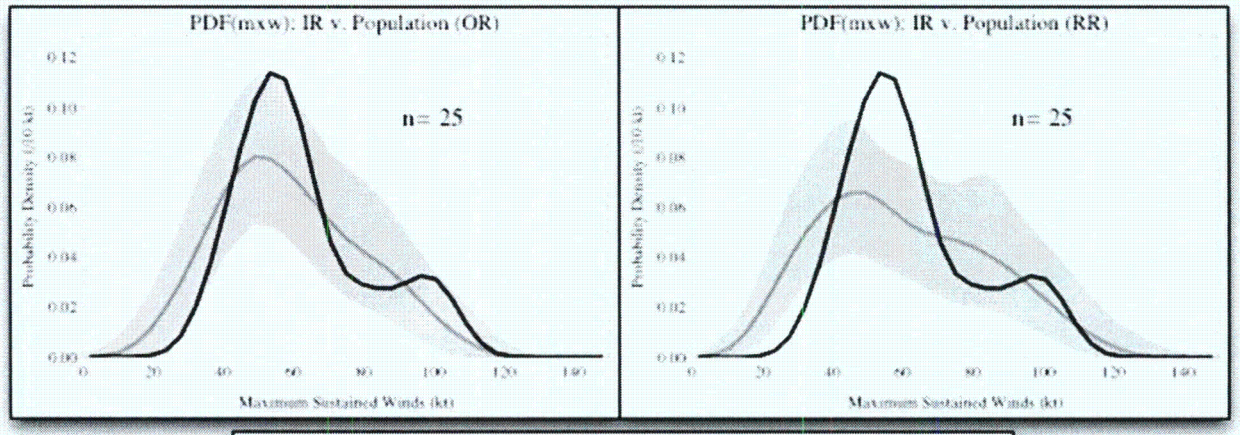

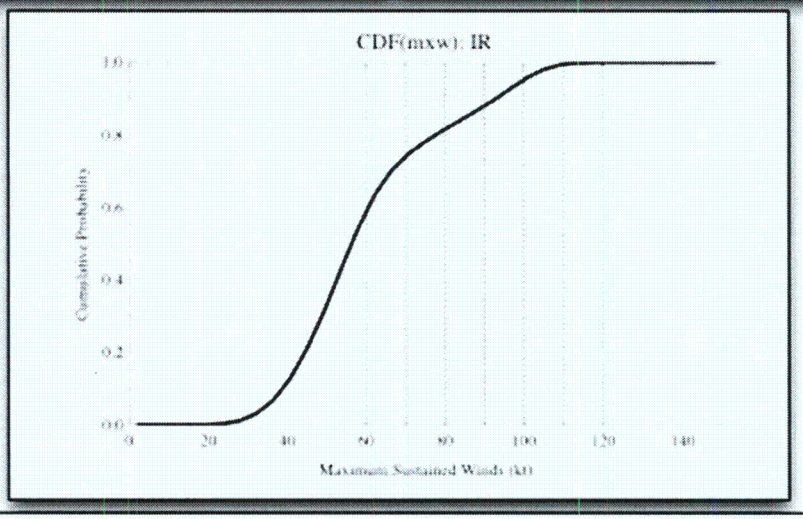

Probability of mxw (per interval of 10 kt)

mxw	60	70	80	90	100	110	120
Pr(mxw)	0.2152	0.099	0.0654	0.0695	0.065	0.0193	0.0012
An. Freq(mxw)	0.1182	0.0544	0.0359	0.0382	0.0357	0.0106	0.0007

Figure 2.4-8: The PDF, CDF, tabulated probabilities and annual frequencies for the fdir parameter within the IR. The envelope PDFs pertain to the OR and RR.

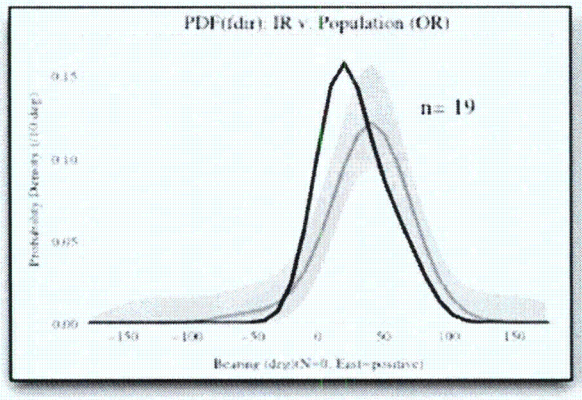

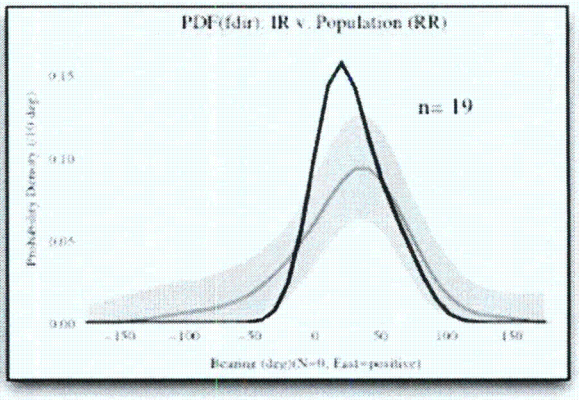

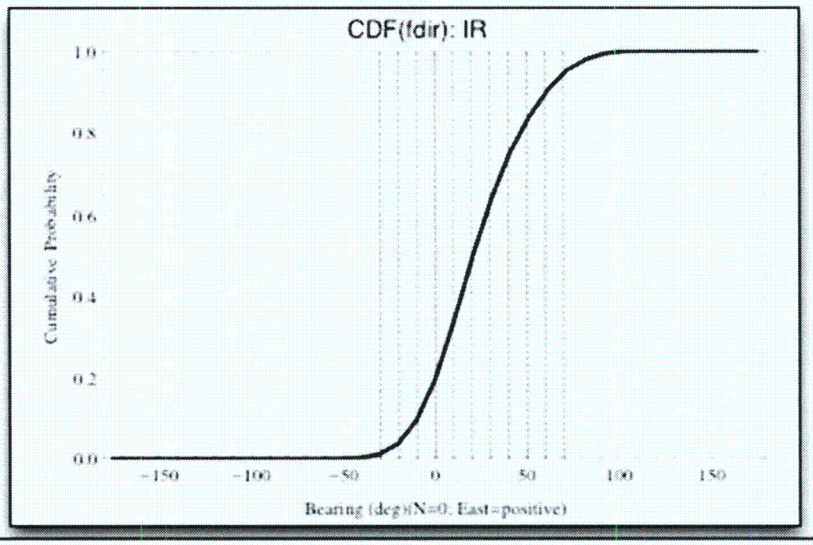

Probability of fdir (per interval of 10 deg)

fdir	-30	-20	-10	0	10	20	30	40	50	60	70
Pr(fdir)	0.018	0.043	0.081	0.121	0.146	0.146	0.126	0.099	0.076	0.057	0.04
An. Freq(fdir)	0.01	0.023	0.044	0.066	0.08	0.08	0.069	0.054	0.042	0.031	0.022

Figure 2.4-9: The PDF, CDF, tabulated probabilities and annual frequencies for the fspd parameter within the IR. The envelope PDFs pertain to the OR and RR.

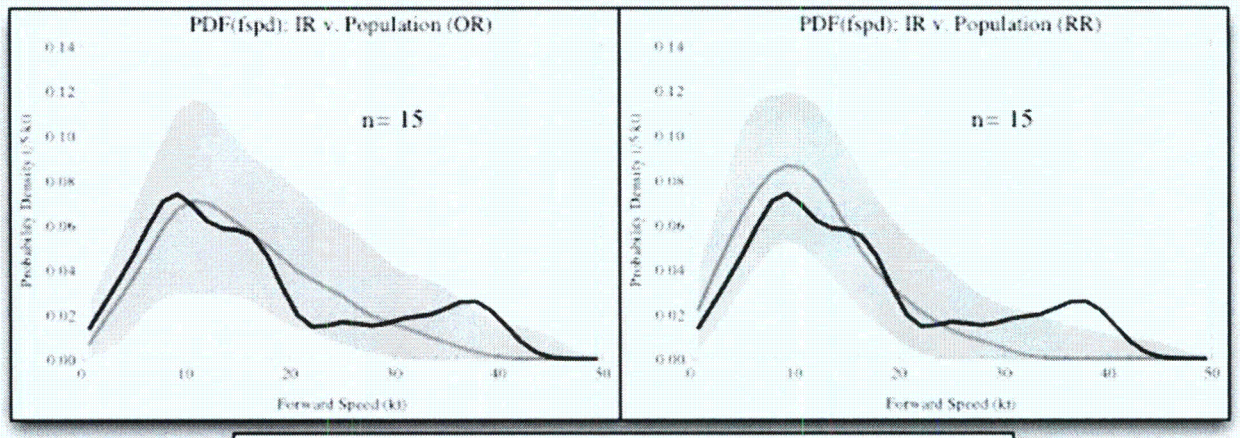

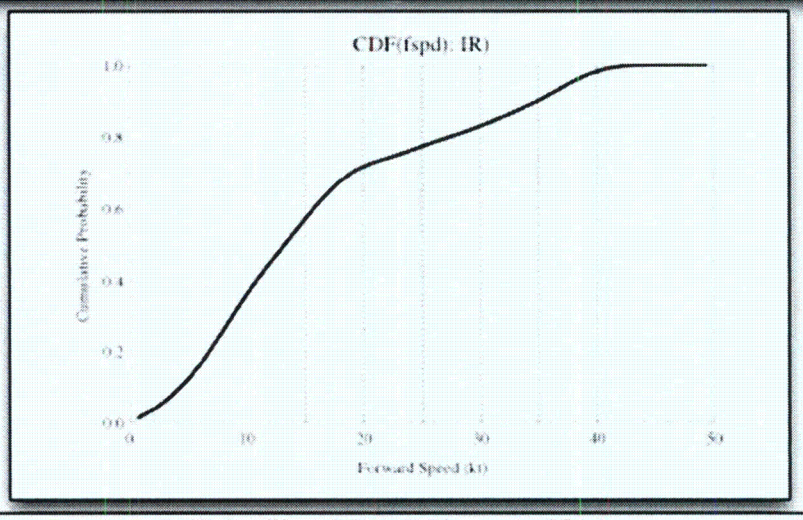

Probability of fspd (per interval of 5 kt)

fspd	15	20	25	30	35	40
Pr(fspd)	0.193	0.081	0.055	0.062	0.083	0.052
An. Freq(fspd)	0.106	0.045	0.03	0.034	0.046	0.028

Figure 2.4-10: The PDF, CDF, tabulated probabilities and annual frequencies for the cpd (central pressure deficit) parameter within the IR. The envelope PDFs pertain to the OR and RR. Only HURDAT2 data from 1979 through 2012 were used to produce these distributions.

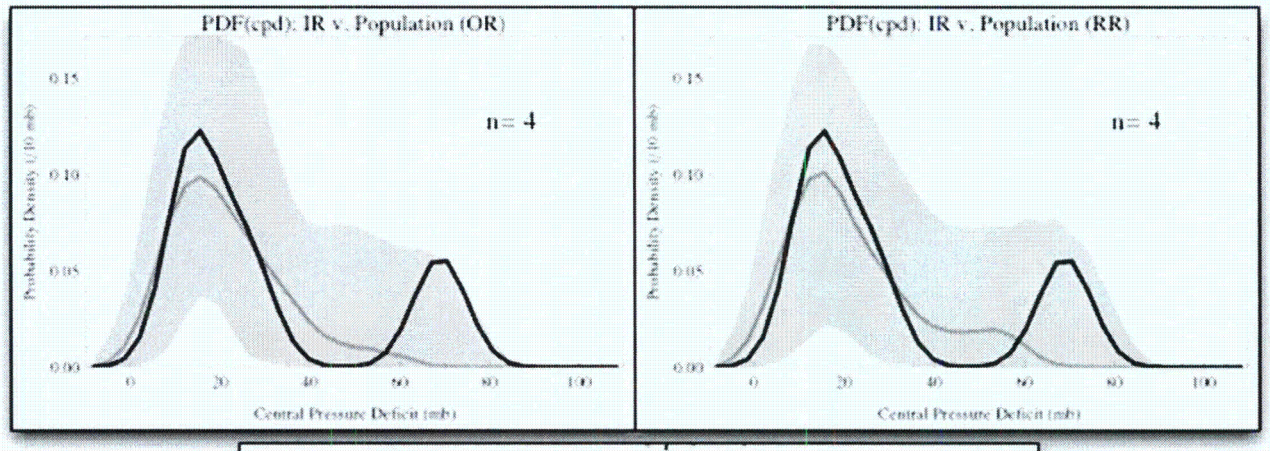

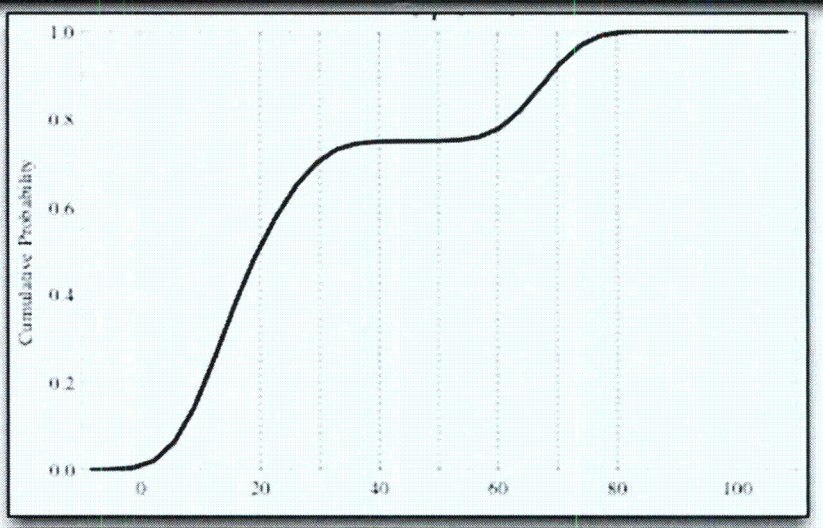

Probability of cpd (per interval of 10 mb)

cpd	20	30	40	50	60	70	80
Pr(cpd)	0.276	0.112	0.069	0.005	0.083	0.138	0.024
An. Freq(cpd)	0.163	0.066	0.005	0.003	0.049	0.081	0.014

Figure 2.4-11: A Probability Density Histogram (PDH) and non-parametric Probability Density Function (PDF) for maximum sustained winds (mxw) within the IR. The inset shows the Gaussian kernel function.

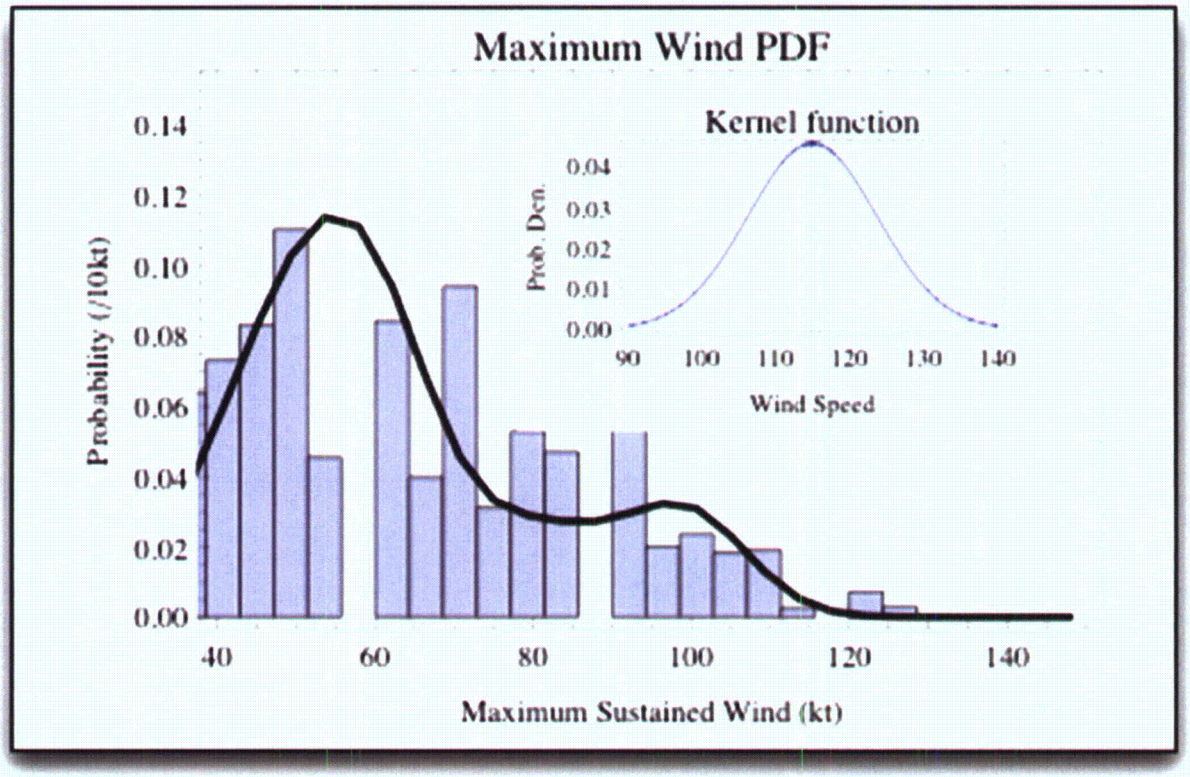

Figure 2.4-12: Hurricane parameter (i.e, mxw, fspd, fdir and dmxw) cross-correlations for the three analytical regions (IR, OR and RR) based on HURDAT2 dataset. Shading indicates statistical significance at the 95% level.

Cross-Correlation (Top=IR; Mid=OR; Bottom=RR)

	mxw	fspd	fdir	dmxw
mxw	1. 1. 1.	-0.02 0.1 0.09	-0.41 -0.15 -0.16	-0.42 -0.18 -0.11
fspd	-0.02 0.1 0.09	1. 1. 1.	0.02 0.1 0.16	0.07 0.08 0
fdir	-0.41 -0.15 -0.16	0.02 0.1 0.16	1. 1. 1.	0.16 0.21 0.05
dmxw	-0.42 -0.18 -0.11	0.07 0.08 0	0.16 0.21 0.05	1. 1. 1.

Figure 2.4-13: Scatter plots of fdir versus fspd data within the three analytical regions for the 162-year HURDAT2 record.

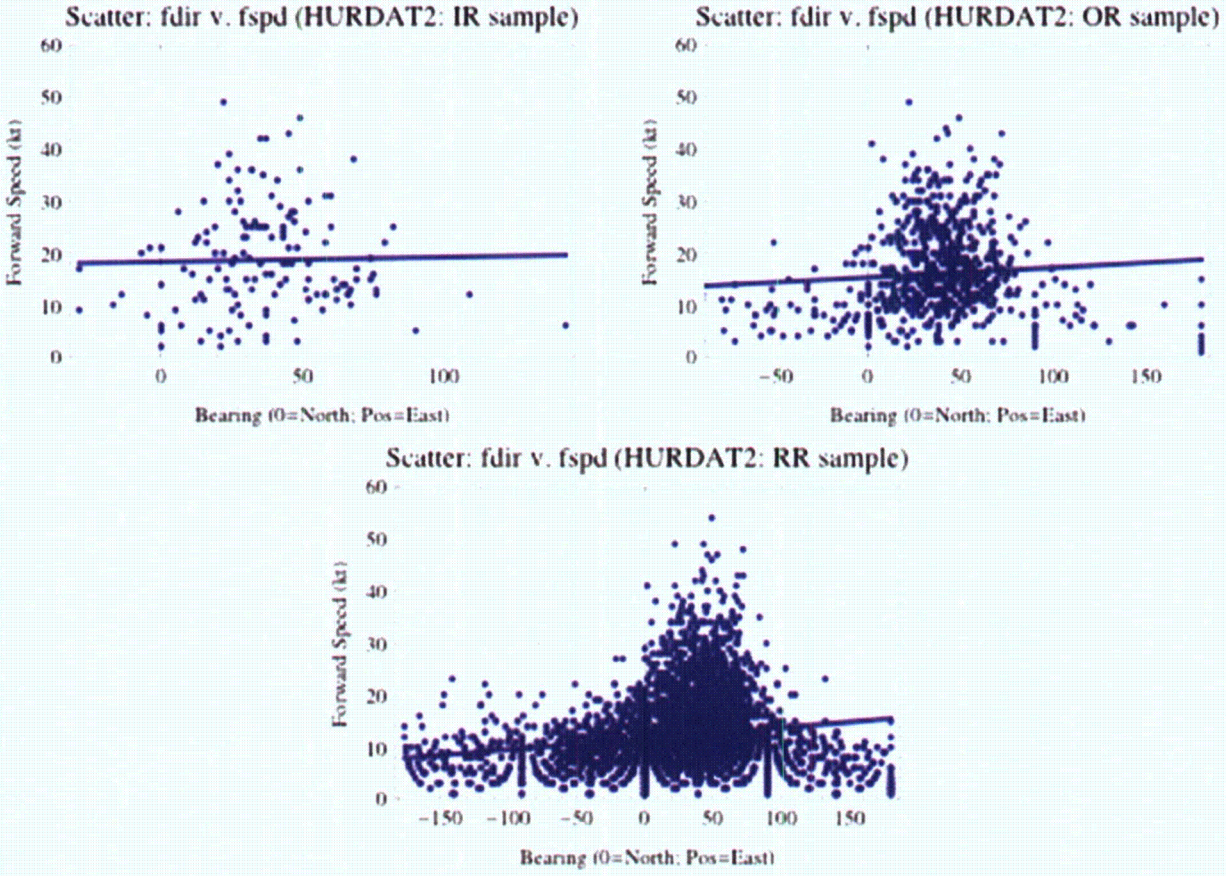

Figure 2.4-14: Scatter plots of fdir versus mxw data within the three analytical regions for the 162-year HURDAT2 record.

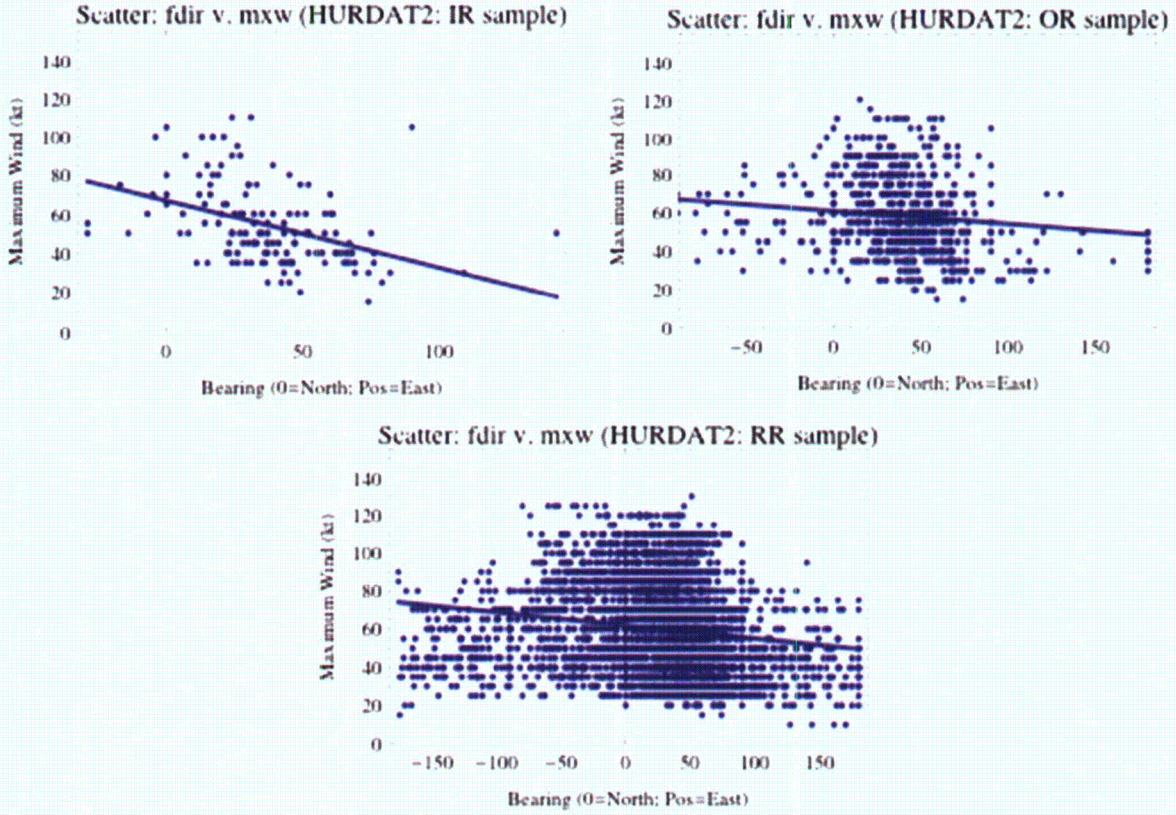

Figure 2.4-15: Scatter plots of mxw versus fspd data within the three analytical regions for the 162-year HURDAT2 record.

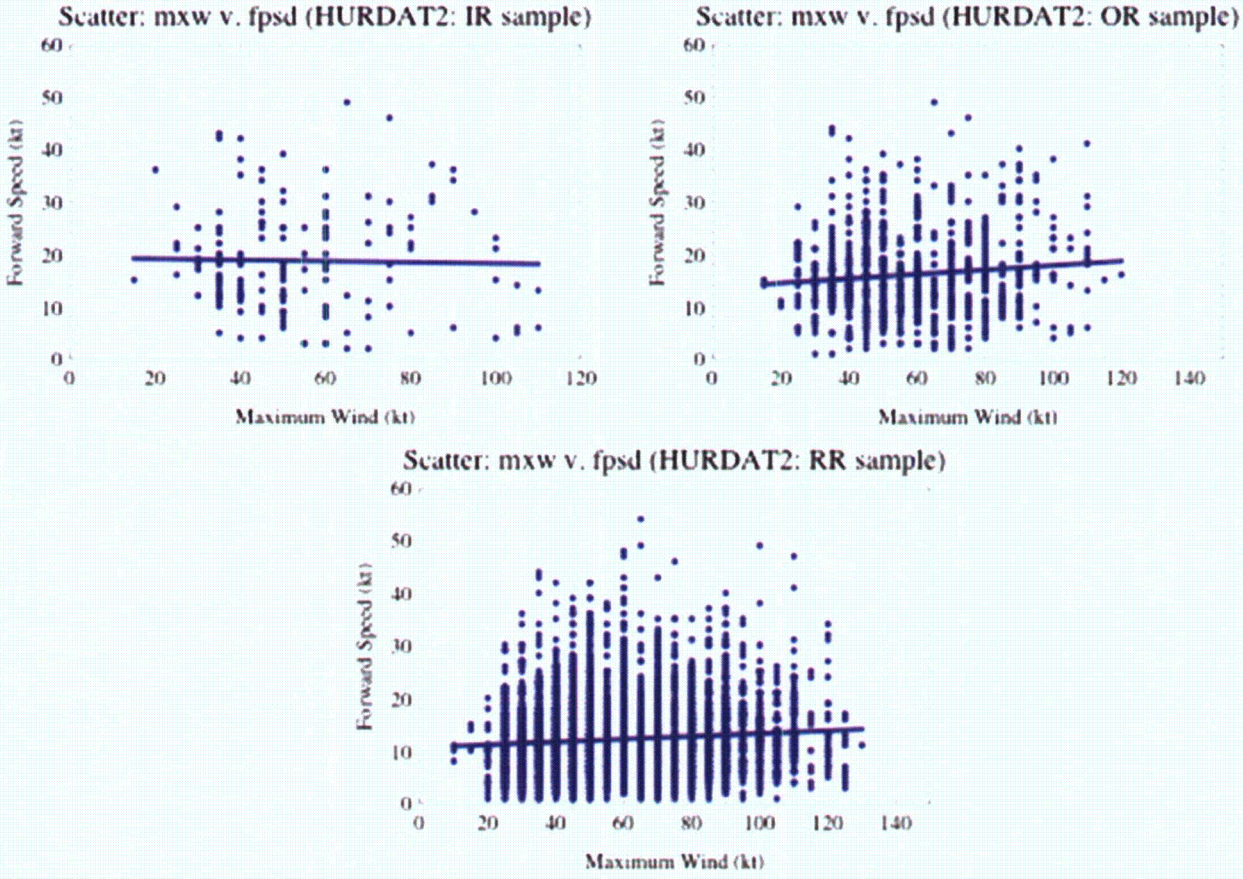

Figure 2.4-16: Scatter plots of fdir versus dmxw data within the three analytical regions for the 162-year HURDAT2 record.

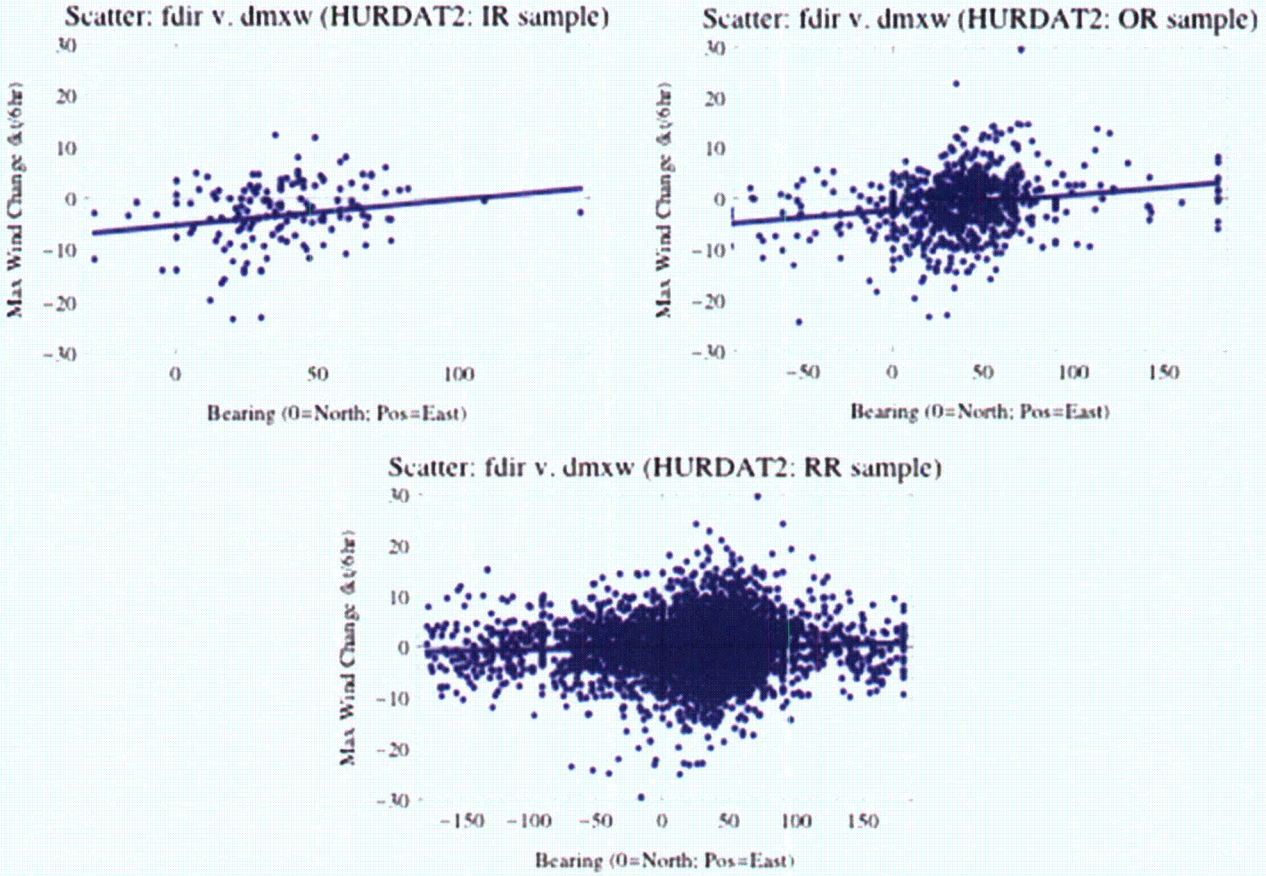

Figure 2.4-17: Scatter plots of mxw versus dmxw data within the three analytical regions for the 162-year HURDAT2 record.

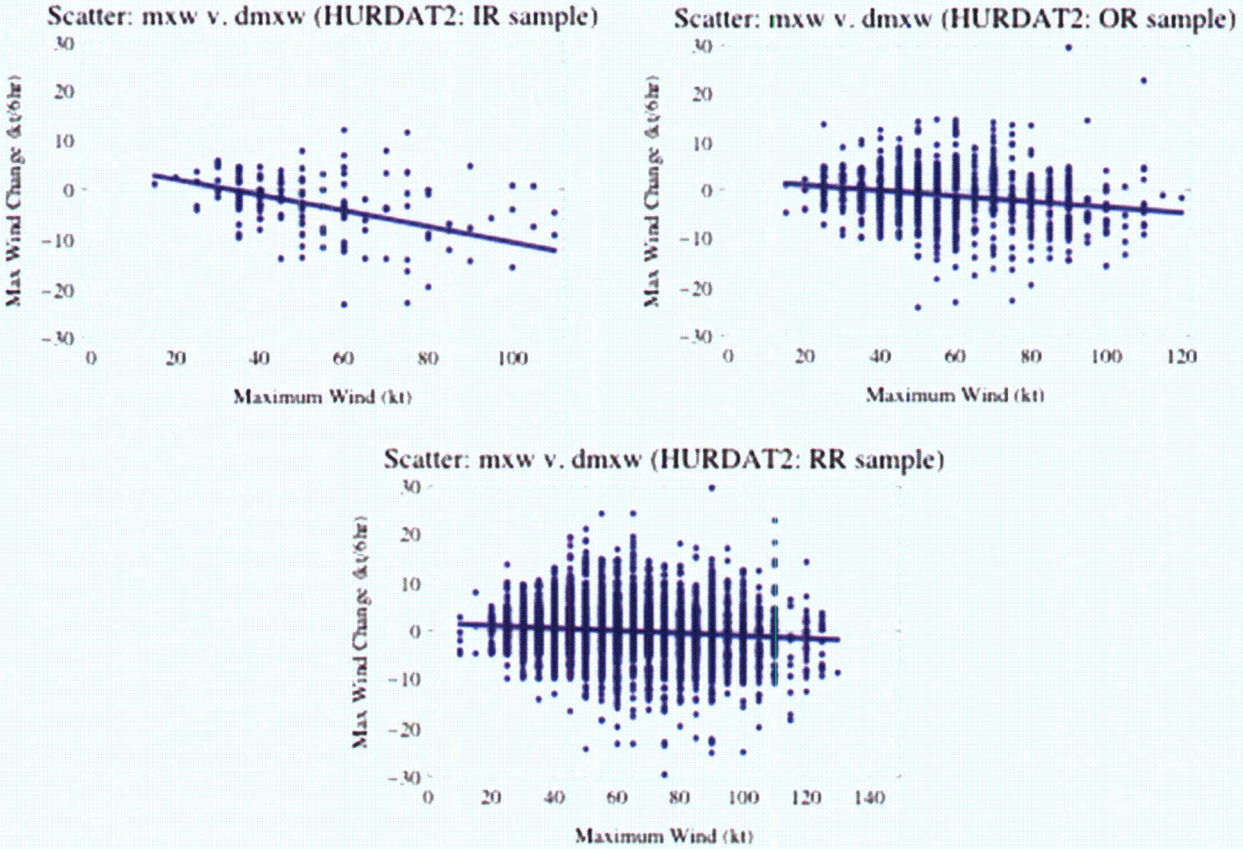

Figure 2.4-18: Scatter plots of fspd versus dmxw data within the three analytical regions for the 162-year HURDAT2 record.

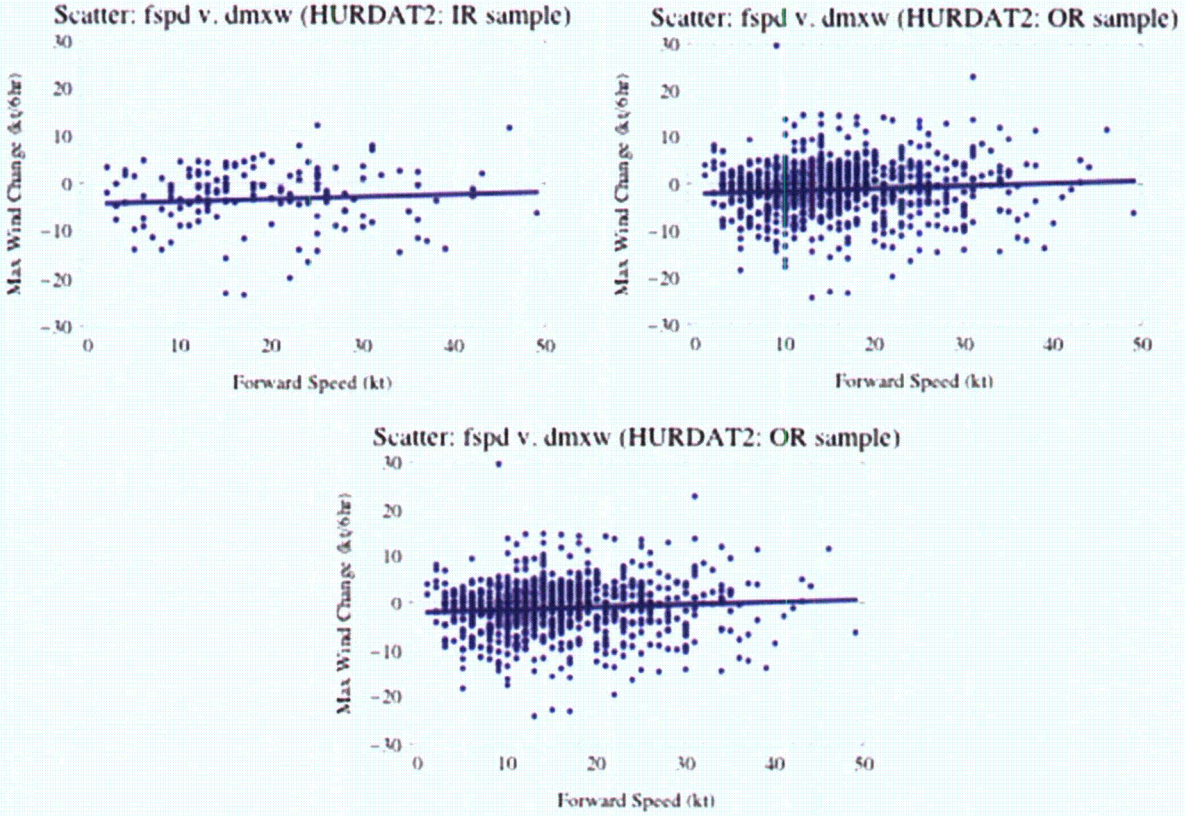

Figure 2.4-19: Comparisons between HURDAT2 distributions of storm bearing (fdir), shown by multiple lines, and the WRT population estimate, shown by gray line surrounded by central 98% uncertainty bounds.

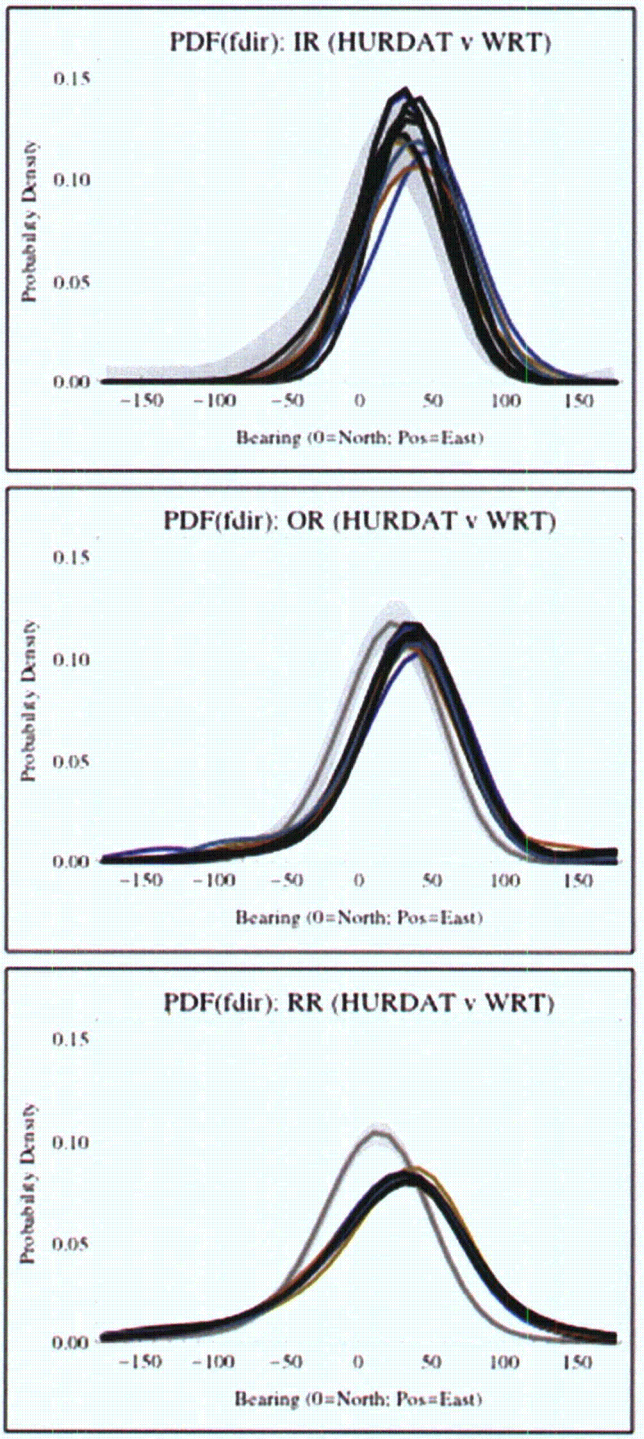

Figure 2.4-20: As in Figure 2.4-19, except pertaining to the storms' translation speed (fspd).

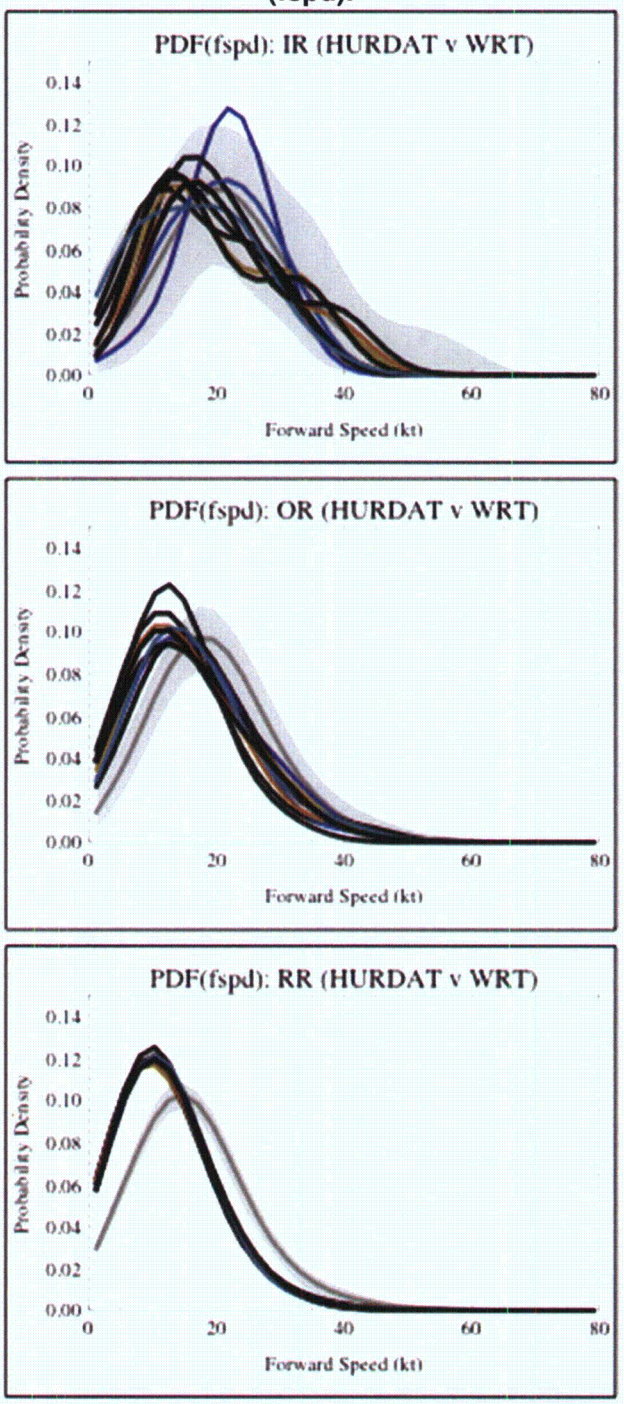

Figure 2.4-21: As in Figure 2.4-19 except pertaining to the storms' change in intensity, as indicated by the 6-hourly change in 1-min maximum sustained winds (dmxw).

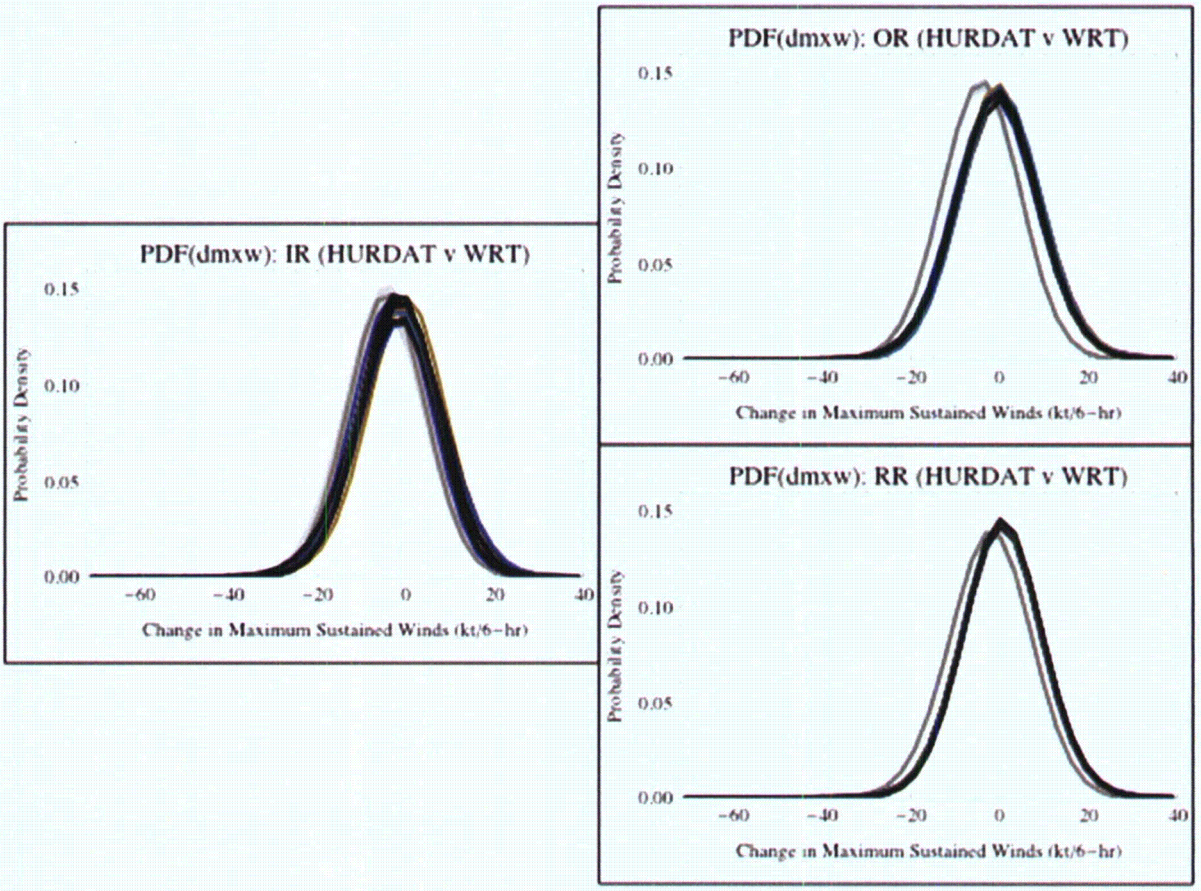

Figure 2.4-22: As in Figure 2.4-19 except pertaining to the 1-minute maximum sustained winds. (as indicated by vm in the WRT data set). The right panels show magnifications of Category 1 at higher hurricanes (upper) and Category 3 and higher hurricanes (lower).

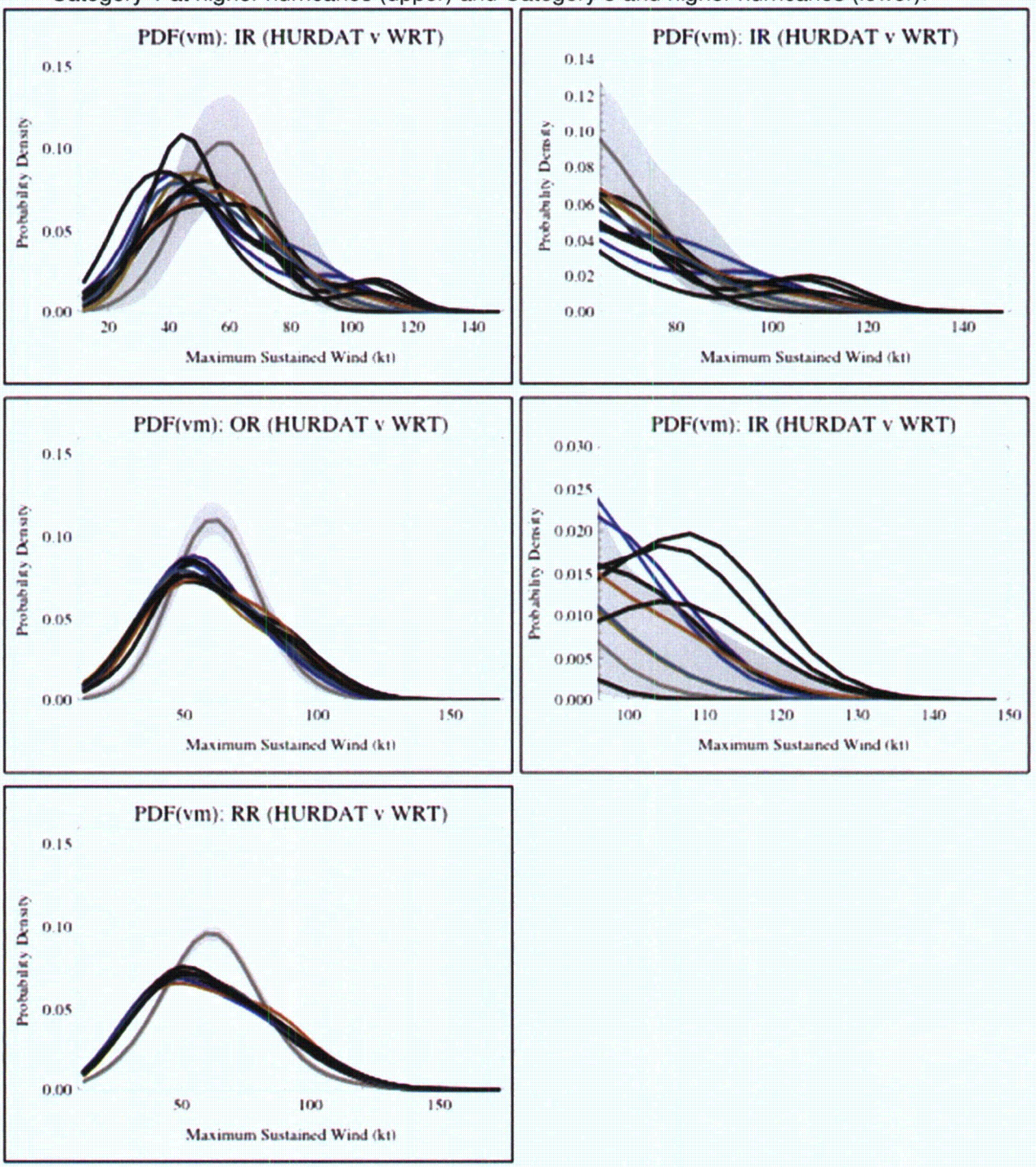

Figure 2.4-23: MPS Circular Region (IR), Offshore Portion and Storm Segment Data

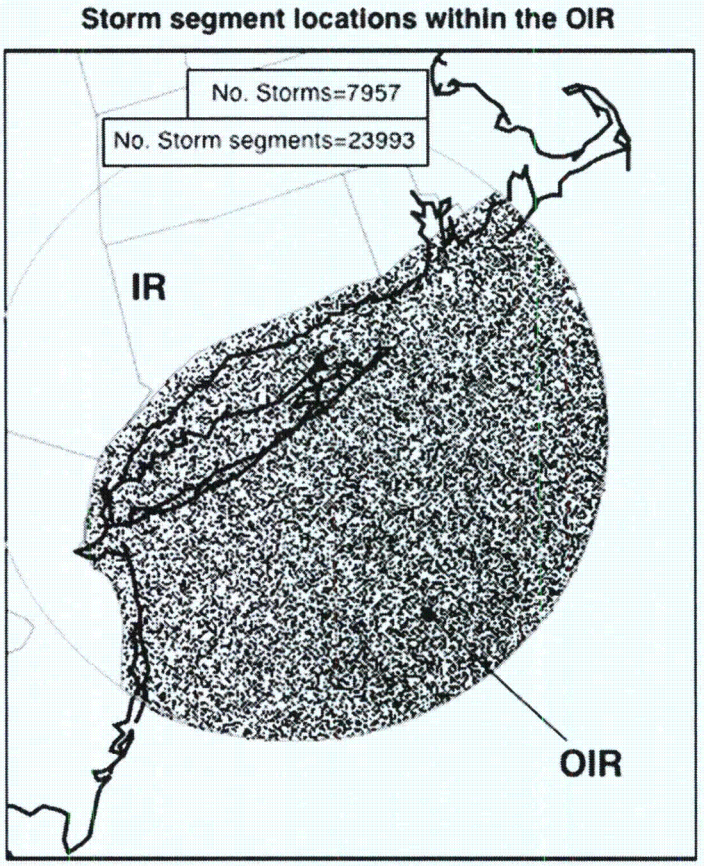

Figure 2.4-24: Annual Frequency of Synthetic Storms by Year and 31-year Averages

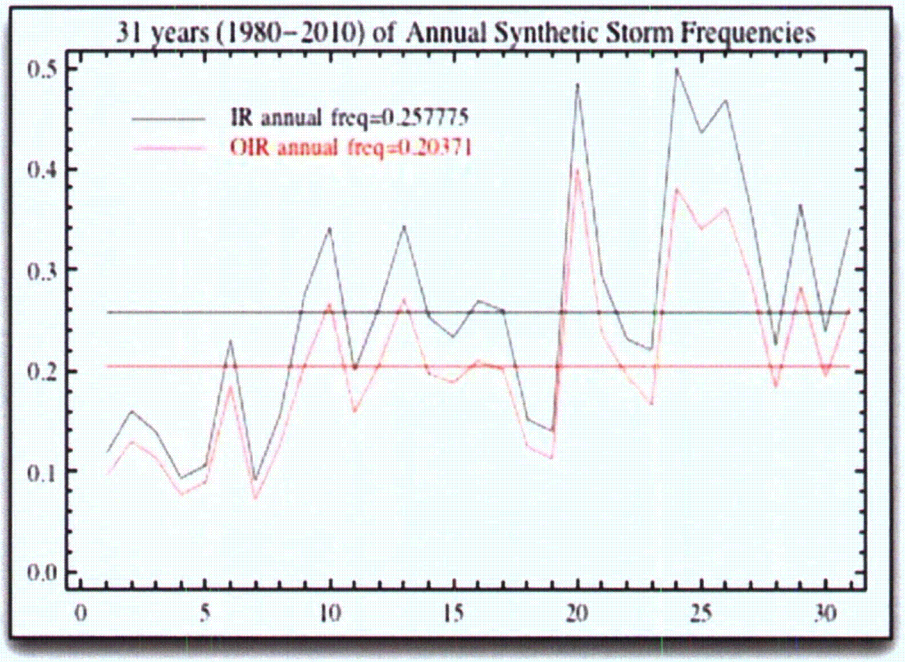

Figure 2.4-25: The PDF, CDF, tabulated probabilities and annual frequencies for the vm parameter within the OIR based on the WRT dataset.

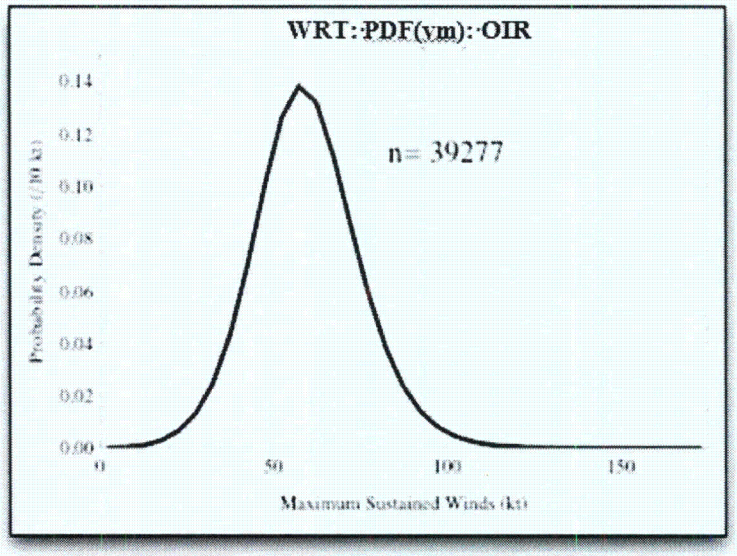

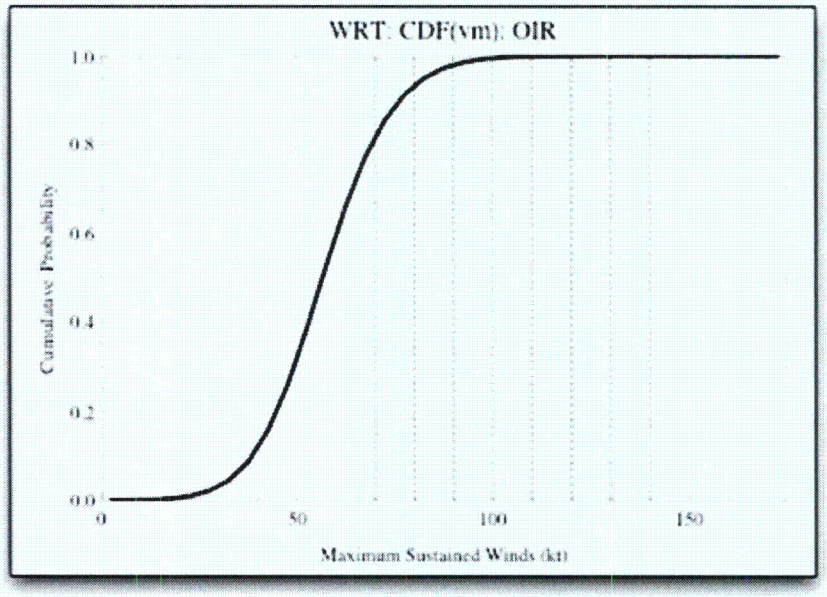

Probability of vm (per interval of 10 kt)

vm	70	80	90	100	110	120	130	140
Pr(vm)	0.16828	0.07627	0.02732	0.00816	0.0022	0.00059	0.00015	0.00004
An. Freq(vm)	0.03428	0.01554	0.00556	0.00166	0.00045	0.00012	0.00003	0.00001

Figure 2.4-26: The PDF, CDF, tabulated probabilities and annual frequencies for the fdir parameter within the OIR based on the WRT dataset.

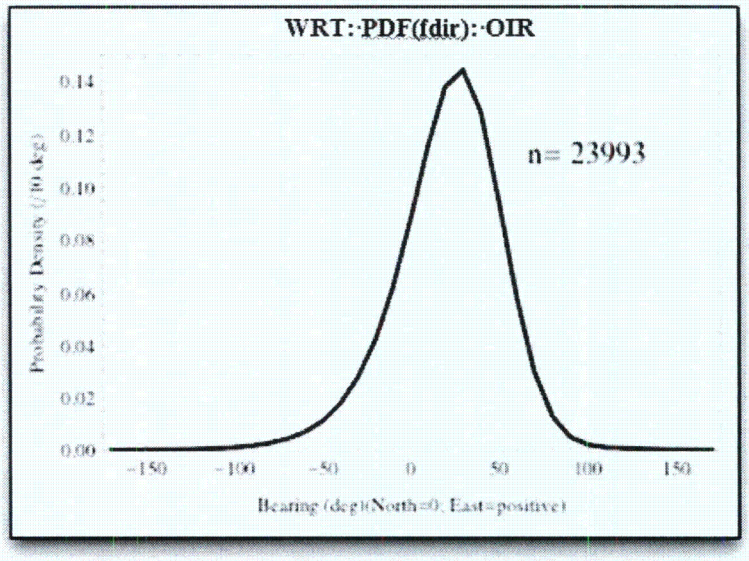

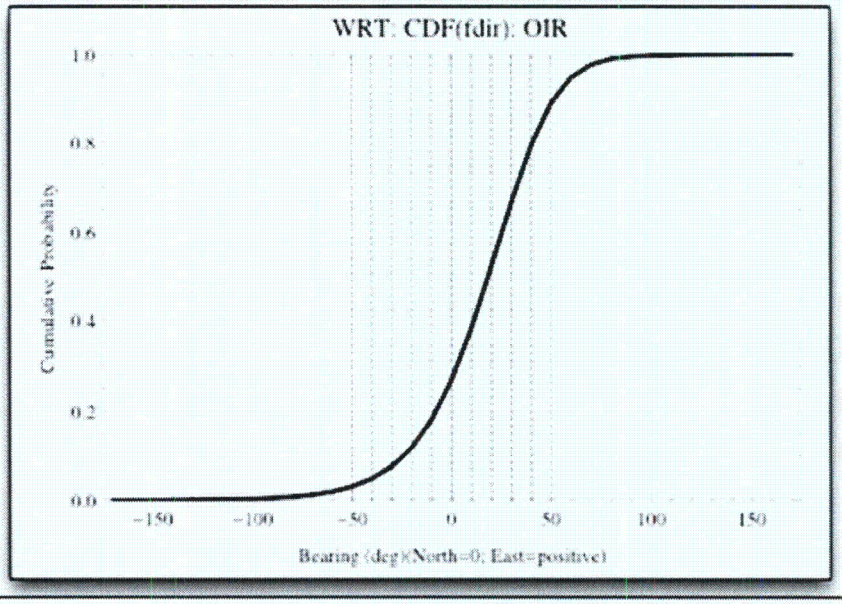

Probability of fdir (per interval of 10 deg)

fdir	−50	−40	−30	−20	−10	0	10	20	30	40	50
Pr(fdir)	0.0141	0.0222	0.0342	0.0513	0.0741	0.1013	0.1277	0.1432	0.1385	0.1129	0.0764
An Freq(fdir)	0.0029	0.0045	0.007	0.0105	0.0151	0.0206	0.026	0.0292	0.0282	0.023	0.0156

Figure 2.4-27: The PDF, CDF, tabulated probabilities and annual frequencies for the fspd parameter within the OIR based on the WRT dataset.

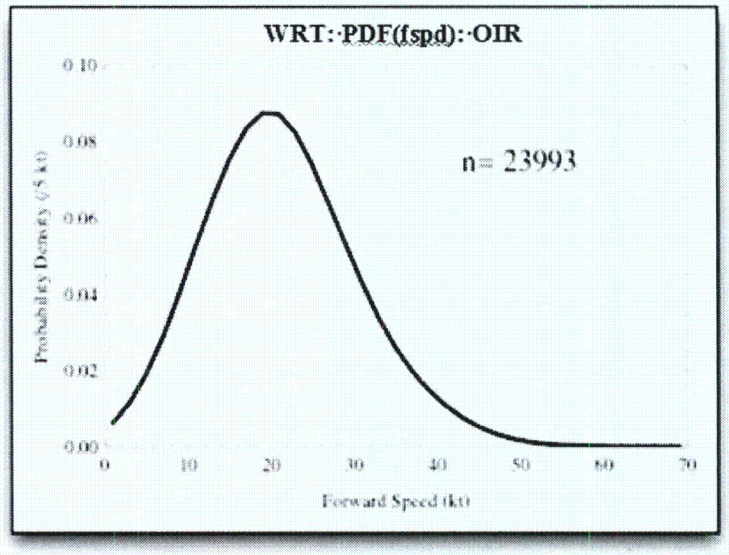

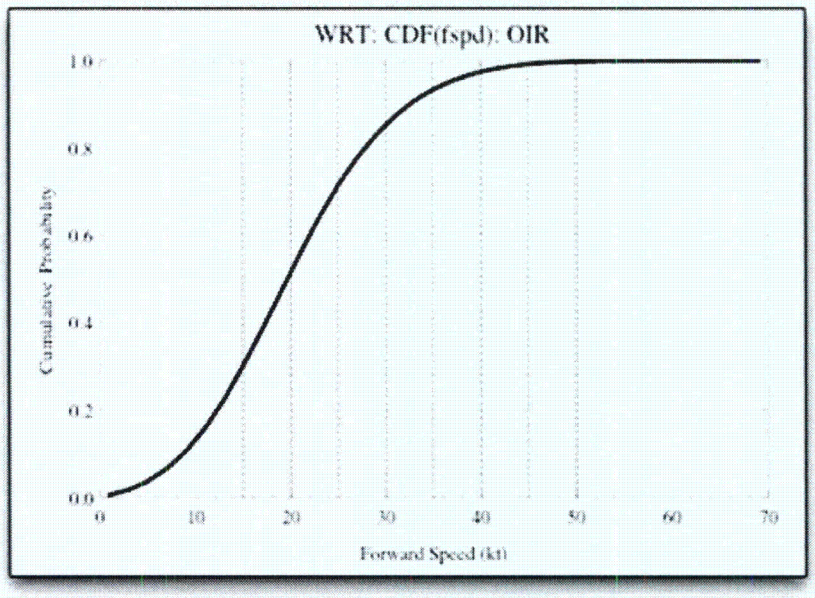

Probability of fspd (per interval of 5 kt)

fspd	15	20	25	30	35	40	45	50
Pr(fspd)	0.1973	0.2152	0.1718	0.1076	0.0577	0.0275	0.0109	0.0034
An. Freq(fspd)	0.0402	0.0438	0.035	0.0219	0.0118	0.0056	0.0022	0.0007

Figure 2.4-28: The PDF, CDF, tabulated probabilities and annual frequencies for the rmw parameter within the OIR based on the WRT dataset.

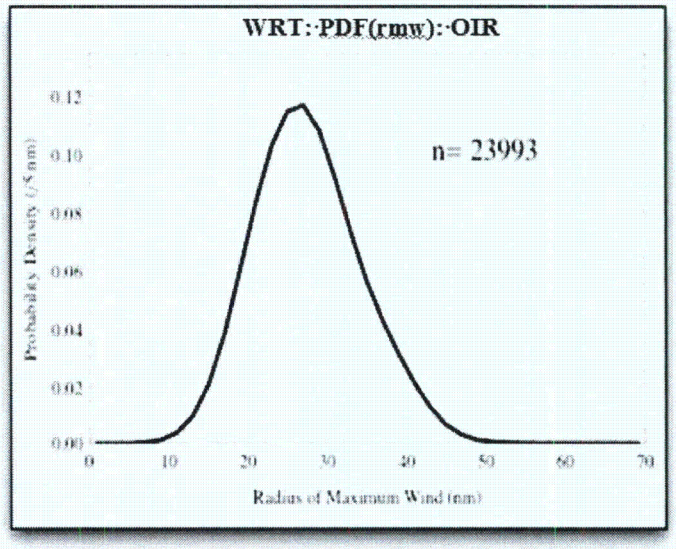

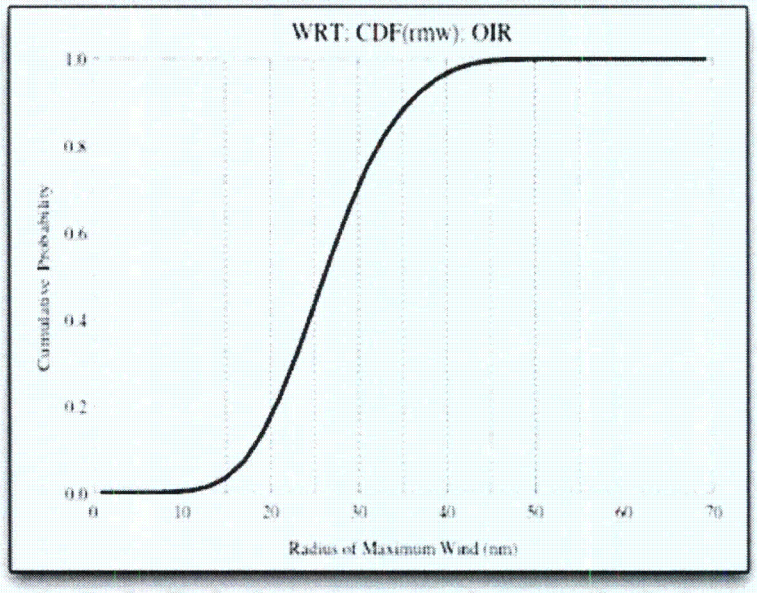

Probability of rmw (per interval of 5 nm)

rmw	15	20	25	30	35	40	45	50	55
Pr(rmw)	0.0751	0.2064	0.2869	0.2282	0.1238	0.0532	0.0124	0.0015	0.0003
An. Freq(rmw)	0.0153	0.042	0.0584	0.0465	0.0252	0.0108	0.0025	0.0003	0.0001

Figure 2.4-29: Storm intensity (vm) extracted from the 3M data set as a function of storm bearing based on the calculated PMH intensity data set rank. The regression line represents a fifth-order polynomial function developed from a least-squares fit to the interval-specific intensity values.

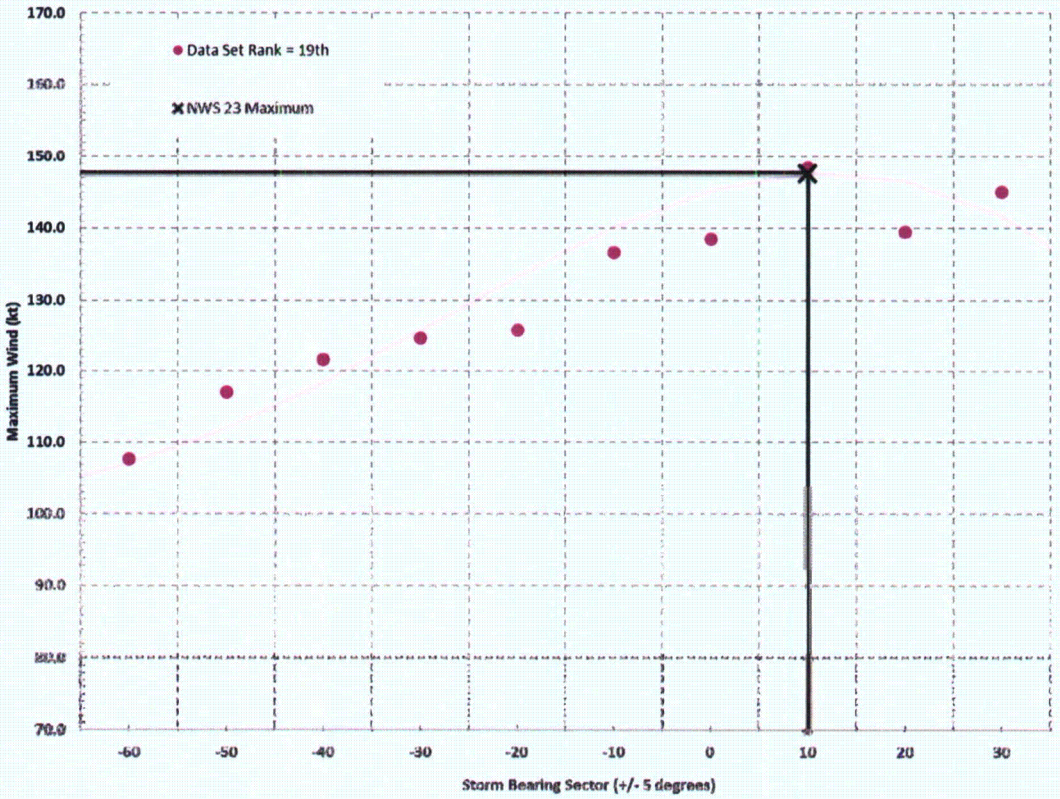

Figure 2.4-30: Scatter plot pairs representing WRT (left panels) and 3M (right panels) data. PMH parameter bounds for storm forward speed (fspd) and radius of maximum winds (rmw) are depicted in red. The limits depicted in the right panels are identical to the limits depicted in the left panels.

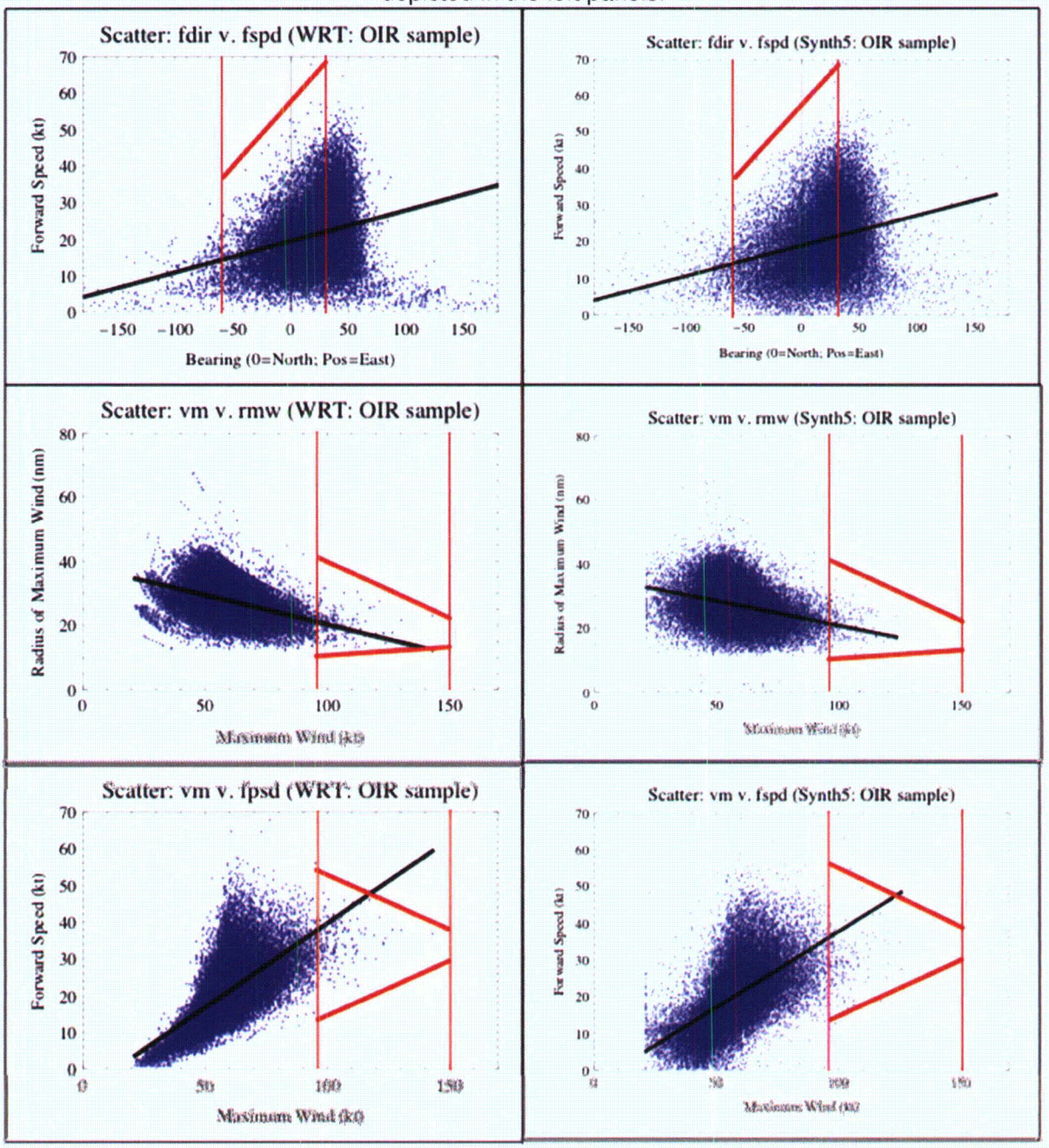

Figure 2.4-31: Simulated storm tracks – bearings ranging from -60° to +30°.

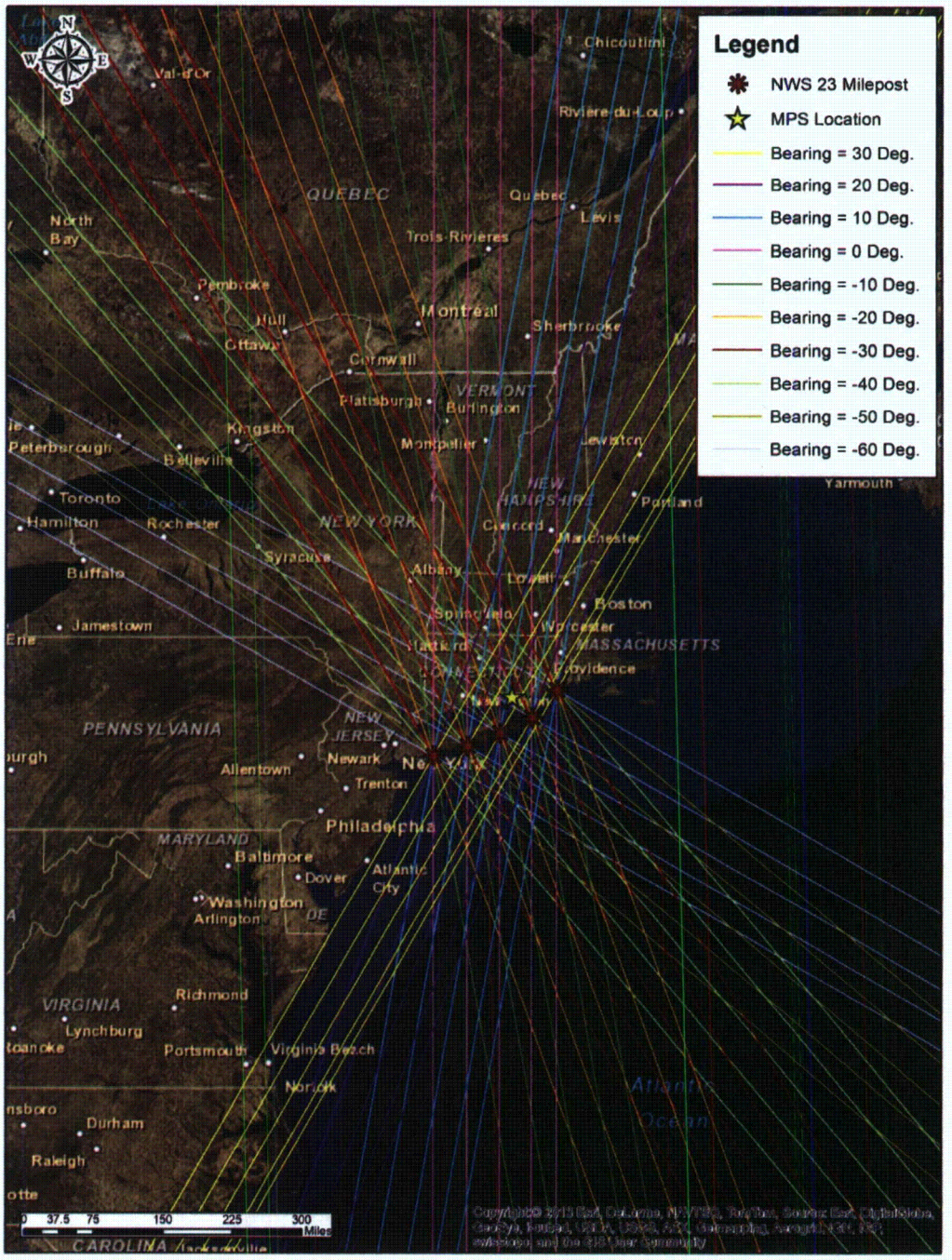

Figure 2.4-32: SLOSH pv2 model basin – MPS vicinity.

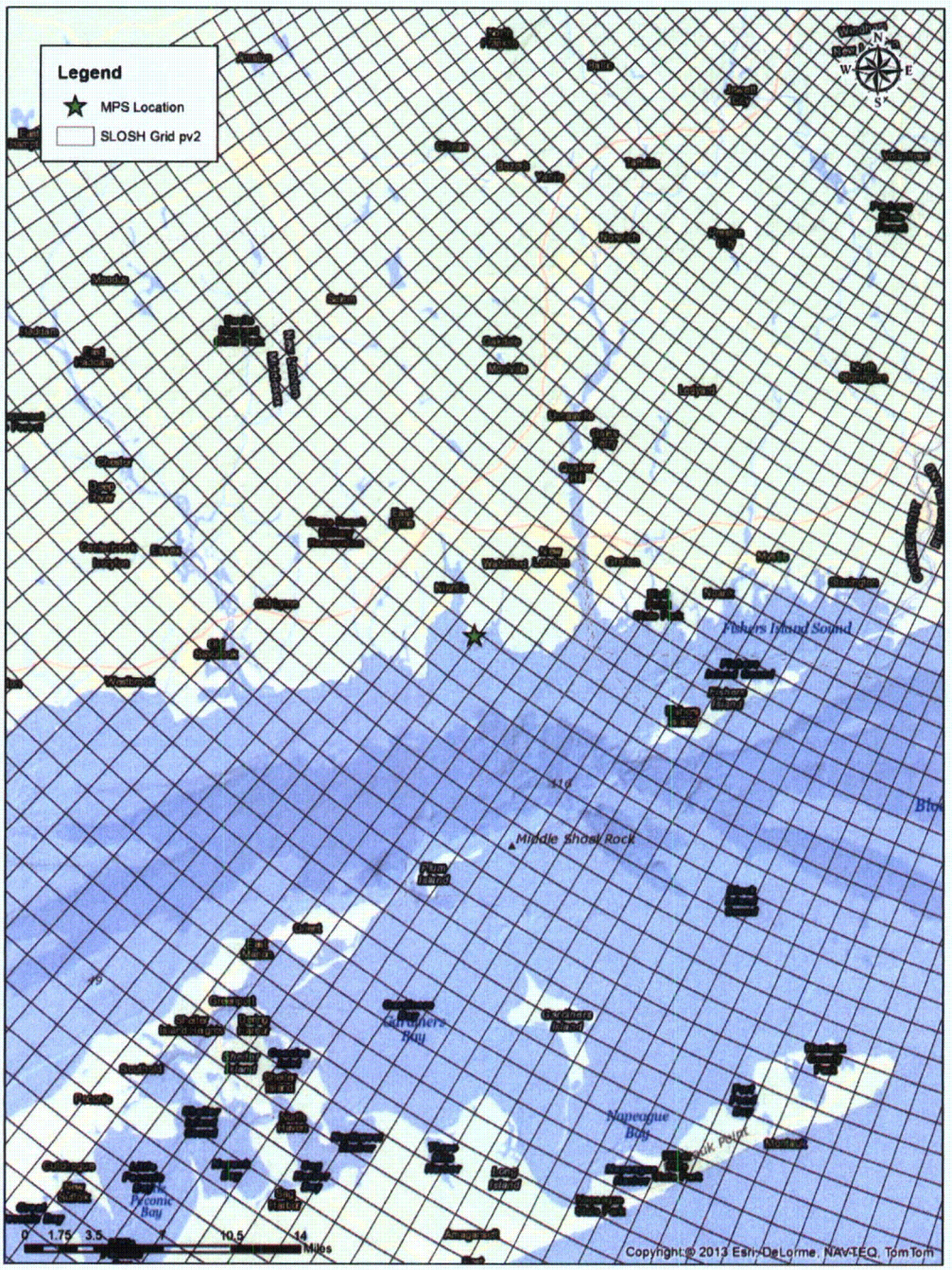

Figure 2.4-33: SLOSH pv2 model basin – MPS region. Cell identifications (i.e., I,J) shown for proximal NOAA tidal gaging and subordinate stations.

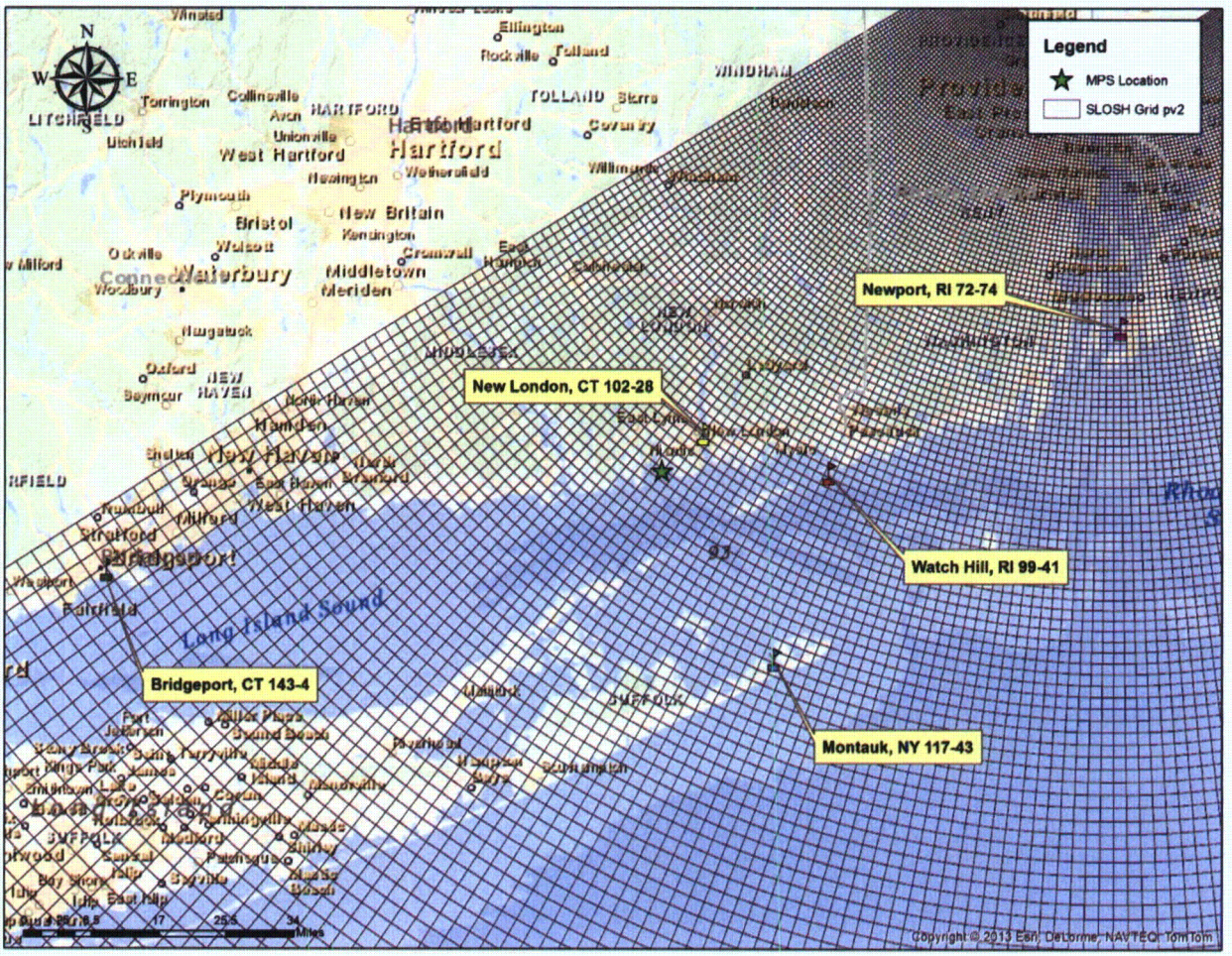

Figure 2.4-34: Screening results – SLOSH-simulated stillwater elevation as a function of storm bearing and forward speed.

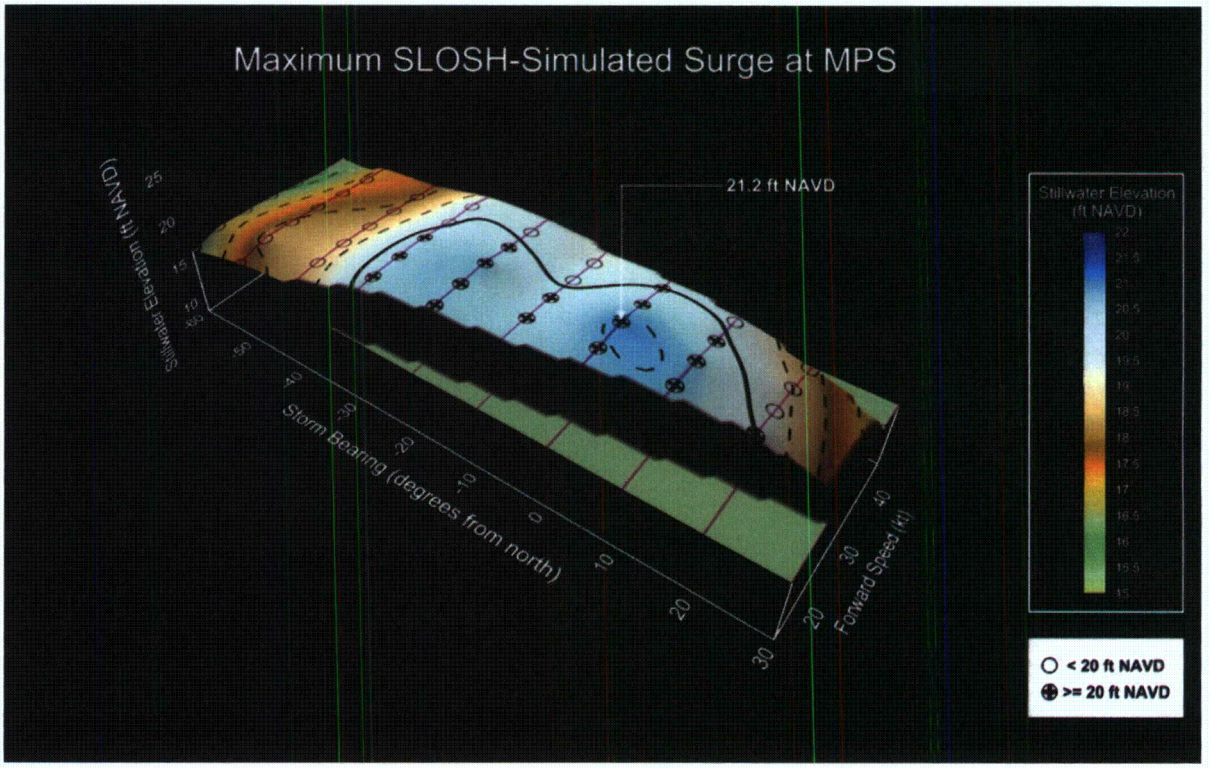

Figure 2.4-35: Screening results – SLOSH-simulated stillwater elevation as a function of storm bearing and radius to maximum winds.

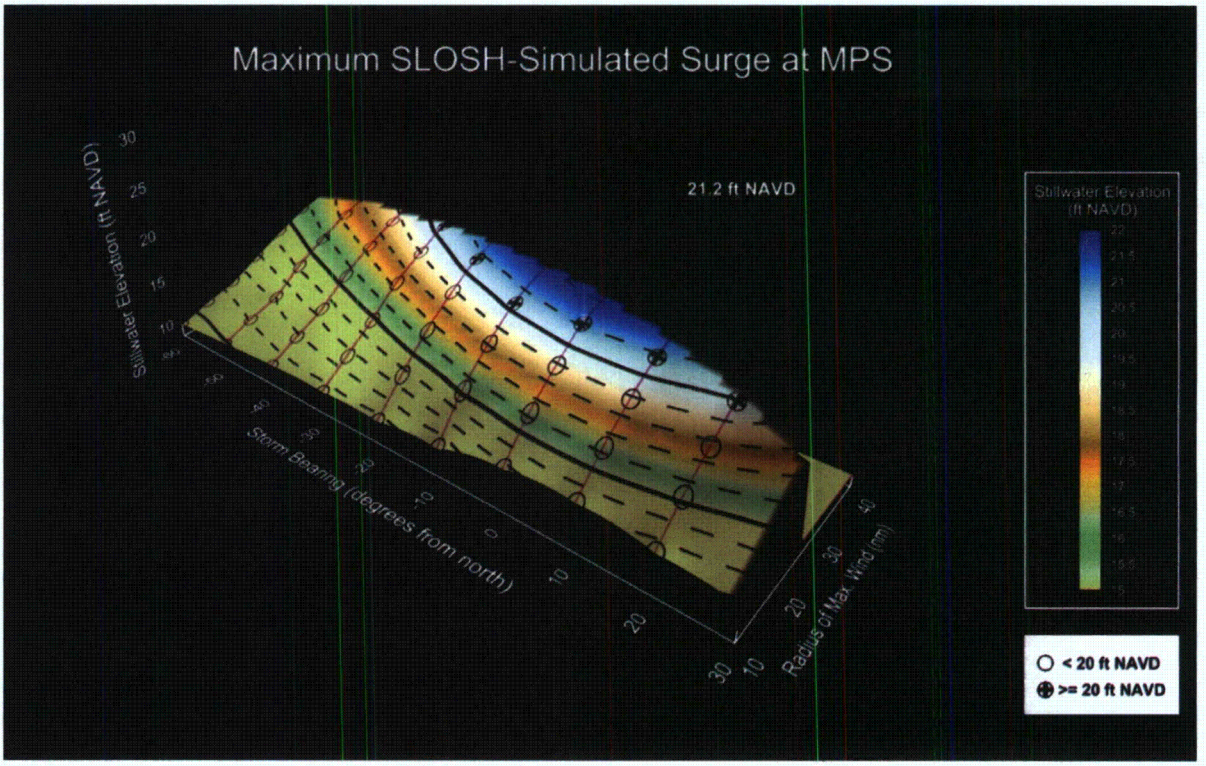

Figure 2.4-36: Simulated storm tracks in the MPS vicinity – bearings ranging from -50° to +50°.

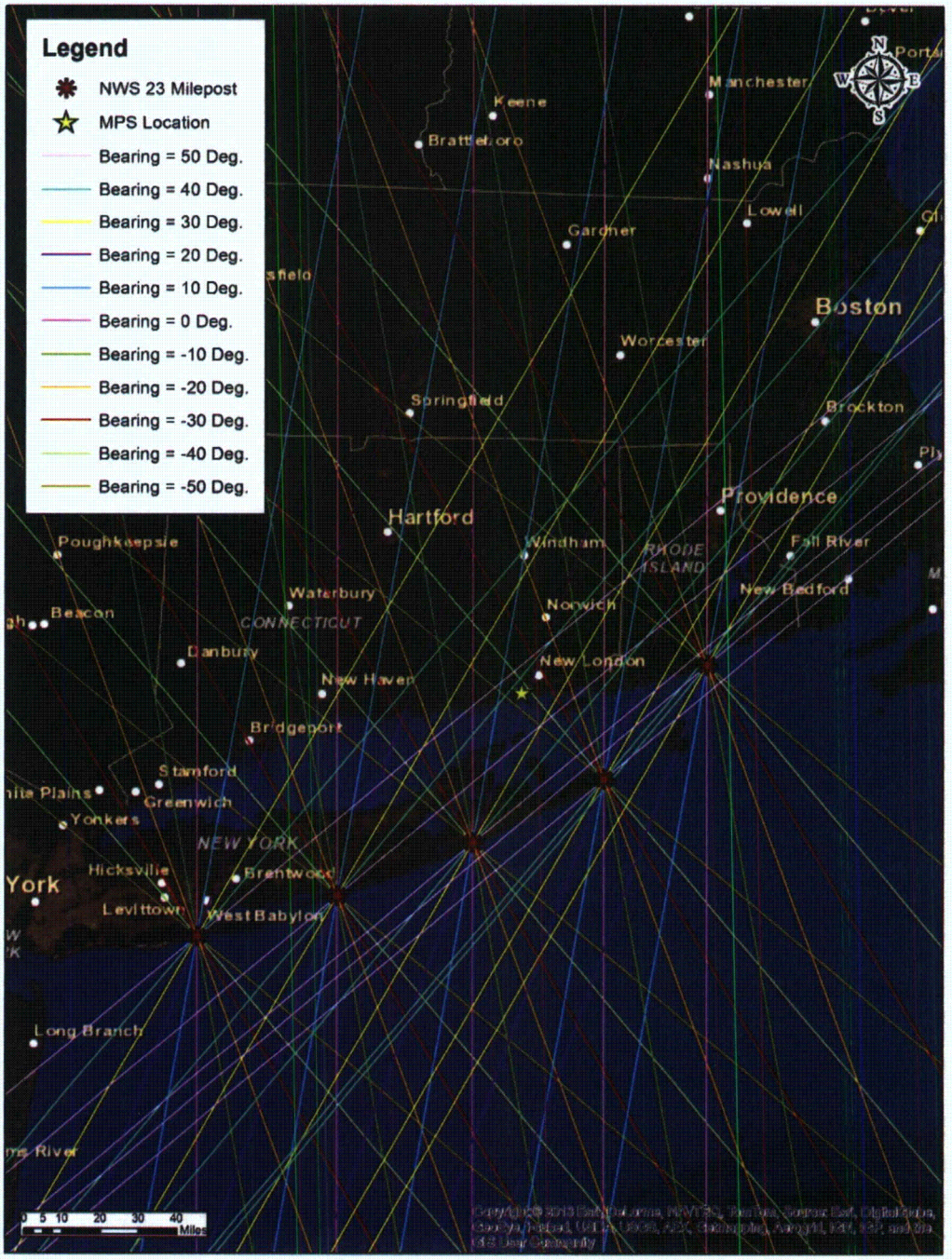

Figure 2.4-37: Comparison of stillwater surge-frequency relationships at MPS developed using the JPM and JPM-OS based on SLOSH results.

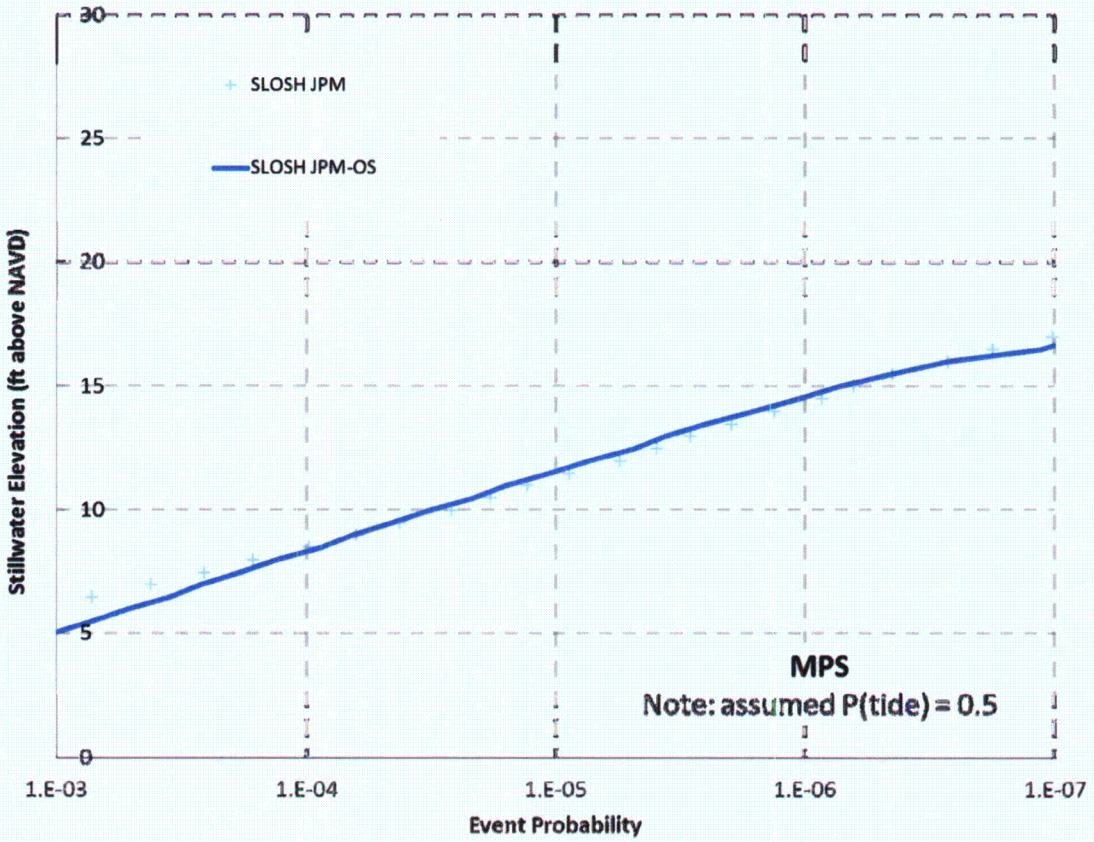

Figure 2.4-38: Refined stillwater surge-frequency relationship at MPS calculated using JPM-OS and ADCIRC including adjustments for uncertainty, error and SLR. The intial JPM / SLOSH and JPM-OS / ADCIRC (no uncertainty or SLR adjustments) relationships are provided for reference. The stillwater surge elevation at an AEP of 1.0E-6 is approximately 19.7 ft NAVD88 with uncertainty, error and SLR considered.

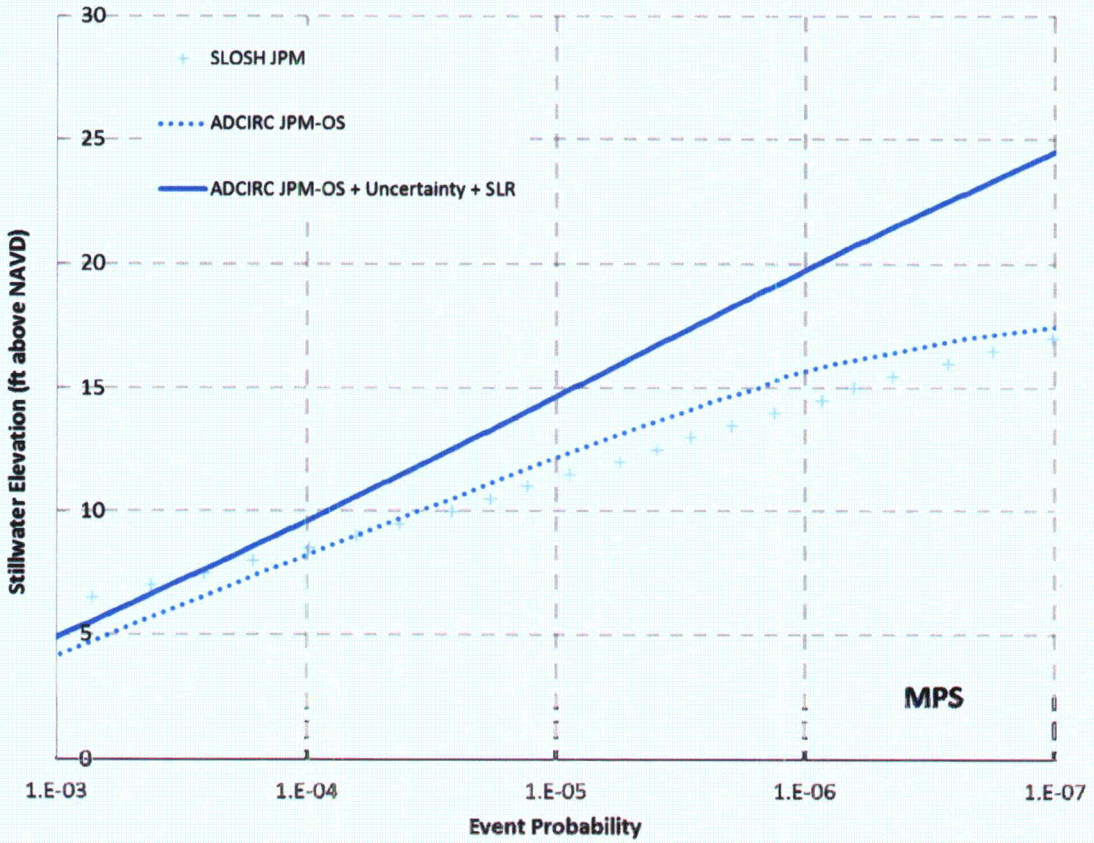

Figure 2.4-39: Refined stillwater surge-frequency relationship (converted to MSL vertical datum) at MPS calculated using JPM-OS and ADCIRC including adjustments for uncertainty, error and SLR. The stillwater surge elevation at an AEP of 1.0E-6 is approximately 20.7 ft MSL with uncertainty, error and SLR considered.